Biochimica et Biophysica Acta 1847 (2015) 399–417

Contents lists available at ScienceDirect

Biochimica et Biophysica Acta

journal homepage: www.elsevier.com/locate/bbabio

Biogenesis of mitochondria in cauliflower (*Brassica oleracea* var. *botrytis*) curds subjected to temperature stress and recovery involves regulation of the complexome, respiratory chain activity, organellar translation and ultrastructure

Michal Rurek [a,*], Andrzej M. Woyda-Ploszczyca [b], Wieslawa Jarmuszkiewicz [b]

[a] Department of Cellular and Molecular Biology, Institute of Molecular Biology and Biotechnology, Faculty of Biology, Adam Mickiewicz University in Poznań, Umultowska 89, 61-614 Poznań, Poland
[b] Department of Bioenergetics, Institute of Molecular Biology and Biotechnology, Faculty of Biology, Adam Mickiewicz University in Poznań, Umultowska 89, 61-614 Poznań, Poland

ARTICLE INFO

Article history:
Received 24 July 2014
Received in revised form 5 December 2014
Accepted 16 January 2015
Available online 21 January 2015

Keywords:
Cold stress
Heat stress
DIGE
Mitochondrial biogenesis
Respiratory chain activity
Mitochondrial ultrastructure

ABSTRACT

The biogenesis of the cauliflower curd mitochondrial proteome was investigated under cold, heat and the recovery. For the first time, two dimensional fluorescence difference gel electrophoresis was used to study the plant mitochondrial complexome in heat and heat recovery. Particularly, changes in the complex I and complex III subunits and import proteins, and the partial disintegration of matrix complexes were observed. The presence of unassembled subunits of ATP synthase was accompanied by impairment in mitochondrial translation of its subunit. In cold and heat, the transcription profiles of mitochondrial genes were uncorrelated. The *in-gel* activities of respiratory complexes were particularly affected after stress recovery. Despite a general stability of respiratory chain complexes in heat, functional studies showed that their activity and the ATP synthesis yield were affected. Contrary to cold stress, heat stress resulted in a reduced efficiency of oxidative phosphorylation likely due to changes in alternative oxidase (AOX) activity. Stress and stress recovery differently modulated the protein level and activity of AOX. Heat stress induced an increase in AOX activity and protein level, and *AOX1a* and *AOX1d* transcript level, while heat recovery reversed the AOX protein and activity changes. Conversely, cold stress led to a decrease in AOX activity (and protein level), which was reversed after cold recovery. Thus, cauliflower AOX is only induced by heat stress. In heat, contrary to the AOX activity, the activity of rotenone-insensitive internal NADH dehydrogenase was diminished. The relevance of various steps of plant mitochondrial biogenesis to temperature stress response and recovery is discussed.

1. Introduction

The plant mitochondrial proteome, which is estimated to include at least 1500 proteins [91], dynamically responds to diverse genetic, environmental and developmental signals [60]. Contrary to the structural variability, the plant mitochondrial genomes encode a limited number of proteins [1]. Taylor et al. [92] estimated that 22% of the stress-responsive organellar proteins in Arabidopsis are localized in mitochondria, but the number of mitochondrial proteins involved in the response to abiotic stress conditions is underestimated. Little is known about the crucial steps required for proper mitochondrial biogenesis and how the balance between coordinated expression of mitochondrial and nuclear genes is altered in the assembly of large supramolecular structures during stress conditions [27,40]. Complex studies integrating proteomic, transcriptomic, metabolomic and other approaches for the elucidation of the biological relevance of plant mitochondrial responses to stress and stress recovery in particular are still limited.

Diverse thermal treatments, which are often accompanied by oxidative stress [66], modulate the expression, activity and interactions of many mitochondrial proteins [82]. These proteins include classical components of the stress response, for instance heat shock proteins (HSPs), including low molecular weight HSPs (15–30 kDa) that protect some respiratory complexes (Cs) from degradation [7,20]; nucleoside

Abbreviations: ACO, aconitase; AOX, alternative oxidase; ATP1, ATP2, ATP6, ATP synthase subunits; BN, blue native; CBB, Coomassie Brilliant Blue; Cs, protein complexes; CI, CII, CIII, CIV, respiratory chain complexes; COX, cytochrome *c* oxidase (complex IV); DIGE, fluorescence difference gel electrophoresis; DSP, dithiobis[succinimidyl propionate]; FtSH, plant metalloprotease; HSP(s), heat shock proteins(s); IDH, isocitrate dehydrogenase; LC-ESI-Q-TOF-MS, liquid chromatography-electrospray ionization-quadrupole-time of flight-mass spectrometry; MPP, mitochondrial processing peptidase; NAD, complex I subunits (mitochondrially encoded); NDH, rotenone-insensitive alternative internal/external NADH dehydrogenase; OXPHOS, oxidative phosphorylation; RCR, respiratory control ratio; QCR, quinol:cytochrome *c* reductase; q-RT-PCR, quantitative reverse transcription PCR; SCs, supercomplexes; SDH, succinate dehydrogenase; State 3, phosphorylating respiration; State 4, non-phosphorylating respiration; TIM/TOM, translocase of the inner/outer mitochondrial membrane; TMPD, *N,N,N′N′*-tetramethyl-*p*-phenylenediamine; VDAC, voltage-dependent anion channel

* Corresponding author. Tel.: +48 61 8295968; fax: +48 61 8295973.
E-mail address: rurek@amu.edu.pl (M. Rurek).

http://dx.doi.org/10.1016/j.bbabio.2015.01.005
0005-2728/

diphosphate kinase [22]; glycine decarboxylase H-protein and other matrix enzymes to be degraded also in oxidative stress [87,89,90]; alternative NAD(P)H dehydrogenases and dehydrin-like proteins [81]. Energy-dissipating components, including alternative oxidase (AOX) and uncoupling proteins (UCP), play a key role in the stress response in plant mitochondria [11,77]. So far, only a few exhaustive studies on the plant mitochondrial proteome under cold and heat stress have been carried out [74,88,90,104].

This work was undertaken to gain a comprehensive view of the influence of temperature stress, including cold and heat, and the recovery from cold and heat, on the biogenesis of cauliflower (*Brassica oleracea* var. *botrytis*) curd mitochondria using proteomic, complexomic, transcriptomic and functional studies. Cauliflower is one of the most important vegetable crops worldwide [32], thus, it is valuable to analyze organellar proteomes of this plant species [8,35,84]. Notably, in our extensive report, we used two dimensional fluorescence difference gel electrophoresis (2D-DIGE) to analyze, for the first time, the detailed responses of the mitochondrial proteome and complexome of a vegetable plant species to temperature stress and stress recovery. Specifically, we studied: (i) the stability of the oxidative phosphorylation (OXPHOS) system and the abundance of OXPHOS proteins; (ii) the transient interactions between respiratory chain Cs; (iii) the *in-gel* activity of respiratory Cs, the activity of the cytochrome and alternative (AOX-mediated) pathways in isolated mitochondria; (iv) respiratory parameters in cauliflower leaves to evaluate the plant physiological status; (v) alterations in the accumulation of AOX isoforms at the proteomic and transcriptomic levels; (vi) changes in the *de novo* synthesis of mitochondrial proteins, and (vii) variations in mitochondrial morphology. On the whole, we investigated the complex nature of the temperature stress responses which allowed us to estimate the role of mitochondria in a higher plant during cold/heat stress and after recovery.

2. Material and methods

2.1. Growth of plant material, temperature stress application and analyses of physiological responses

Seeds of cauliflower (*B. oleracea* var. *botrytis*) cultivar 'Diadom' were purchased from Bejo Zaden (Poland). The plants were grown for 3 months in cultivation chambers at a local breeding station (University of Life Sciences, Poznan, Poland) at 23/19°C (day/night) and 70% relative humidity under photon flux density 200 μmol m^{-2} s^{-1} (16 h of light/8 h of dark). Stress conditions were applied to the plants with young curds (approximately 10 cm-diameter curds). Cold stress (8°C) and heat stress (40°C) was applied to growing plants for 10 days and 4 h, respectively. After termination of the given stress treatment, some of the cauliflower plants were transferred to standard growth conditions for 48 h (stress recovery). The curds were harvested either immediately after the termination of the stress treatment or after the completion of stress recovery.

Physiological analyses were conducted on well-developed cauliflower leaves using the LI-6400 XT infrared gas analyzer (Li-Cor). The rate of leaf respiration in the light (day respiration) was determined according to the Laisk method [51]. CO_2 assimilation rate representing a given total respiration rate was recorded during intercellular CO_2 concentration (C_i) decreased to 0 ppm at 22°C and 50% relative humidity. For each value of photon flux density at 200, 400 and 600 μmol m^{-2} s^{-1}, 1, the linear regression of CO_2 assimilation (A) versus C_i was calculated and the photorespiration rate was determined as difference between total and day respiration (the latter one expressed as a given CO_2 evolution rate at the crossing point of all A/C_i curves). Duration of the heat stress was estimated on the basis of temperature measurements of cauliflower curds as well as the leaf surface. When heat stress reached up to 40°C, plant surface temperature increased and remained stable for 2 h. After the completion of this period, plants were heat-stressed for further 2 h (4 h in total). Such treatment appeared necessary for the visible increase in the respiration and photorespiration rates (Supplementary Fig. 1). However, when heat stress exceeded 4 h, the leaf turgor decreased and was accompanied by visible rising lesion symptoms, including leaf yellowing and the necrosis during further cultivation days. At 8°C, physiological responses of cauliflower plants were evident after 8 h of cold stress (Supplementary Fig. 1). At this temperature, only physiological parameters, including day and total respiration, and photorespiration rates were significantly decreased. Exposure to cold for 10 days was necessary to observe proteomic and functional alterations. Similarly, the duration of the stress recovery was also optimized in order to detect the significant proteomic and functional changes.

2.2. Isolation of mitochondria, purity assays and protein determination

Mitochondria from the topmost 5-mm-thick layer of the cauliflower curds were isolated by differential centrifugation and purified in Percoll gradients according to Pawlowski et al. [69]. During isolation, the Complete Mini EDTA-free Protease Inhibitor Cocktail (Roche) was added. Purity assays of the isolated mitochondria were conducted according to Rurek [81] and Pawlowski et al. [69]. The protein content was determined using the BioRad Protein Assay, using bovine serum albumin as a standard curve calibrator. The efficiency of the mitochondria preparation was 4–6 mg of mitochondrial proteins per 100 g of cauliflower curds.

2.3. Crosslinking assay

Mitochondria (100 μg) were suspended in a washing medium without bovine serum albumin [81] to a final protein concentration of 1 mg ml^{-1}. Dithiobis[succinimidyl propionate] (DSP, Pierce) that was freshly dissolved in *N*,*N*-dimethylformamide (DMF; Sigma) was added to final concentrations of 0.125, 0.25 and 0.5 mM to act as a crosslinker. Crosslinking was carried out for 2 h at 4°C, and then 10 mM Tris–HCl (pH 7.5) was added. After a subsequent incubation (4°C, for 15 min), the mitochondria were pelleted and the respiratory Cs were analyzed by blue native polyacrylamide gel electrophoresis (BN-PAGE).

2.4. BN-PAGE

Pelleted mitochondria (50–100 μg) were suspended in a 6-aminocaproic acid (ACA) solution [28]. For solubilization (4°C, for 30 min), digitonin (Fluka) was used (4 g of detergent per 1 g of proteins). After centrifuging to separate the non-solubilized material (at 18,300 ×*g*, for 20 min, 4°C), Blue G (Serva) was added to the obtained supernatant. BN-PAGE was carried out according to a modified protocol from Giegé et al. [28] using a mini-gel system from Biometra (5–13% polyacrylamide 10 × 10 cm, 1.5 mm-thick gels). The gels were run at 60 V for 45 min and then at 250 V for 3 h with the current limited to 25 mA (all steps at 4 °C).

2.5. In-gel activity assays

NADH dehydrogenase activity, including the activity of complex I (CI), was detected using a method modified from Zerbetto et al. [105] in a presence of 0.14 mM NADH, 1 mg ml^{-1} nitroblue tetrazolium, 0.1 M Tris–HCl (pH 7.4). Complex II (CII) activity was detected in reaction medium (50 mM phosphate buffer, pH 7.4, 84 mM succinate, 0.2 mM phenazine methosulfate, 2 mg ml^{-1} nitroblue tetrazolium, 4.5 mM EDTA, 10 mM cyanide) according to Jung et al. [44]. Complex IV (CIV) activity (also modified from [105]) was detected in a presence of 10 mM phosphate buffer (pH 7.4), 1 mg ml^{-1} diaminobenzidine, 75 mg/ml sucrose, 19 U ml^{-1} catalase and 16 mM cytochrome *c*. F_0F_1 ATP synthase activity [95] was determined overnight in 50 mM HEPES, pH 8.0, 10 mM ATP and 30 mM $CaCl_2$. All assays were

performed directly on BN gels within the linear range (50–100 μg of proteins) at 25°C in 25 ml and they were stopped by transferring the gels to a fixing solution (40% methanol, 10% acetic acid). The acquired signals were analyzed using Multi Gauge (v.2.2).

2.6. 2D DIGE (BN/Tricine-SDS-PAGE) experimental design

CyDye DIGE minimal dyes (GE Healthcare) and G-Dyes (NH DyeAGNOSTICS) were used. All experiments were conducted in triplicate. Mitochondrial proteins (100 μg or 50 μg) from (i) control, (ii) heat-stressed, and (iii) heat-recovered plants were labeled either with (1) Cy2 or G-Dye200, (2) Cy3 or G-Dye300 and (3) Cy5 or G-Dye300, respectively. G-Dye100 was used to label the internal standard (equivalent of 17 μg of all variants pooled together). An abundance of subunit-β of ATP synthase was also used to equalize the amounts of the compared subproteomes within each experiment. The solubilization of the pelleted mitochondria lasted for 20 min at 4 °C in the presence of 5–20 μl of buffer (pH 7.4) [37] supplemented with 5% digitonin. After removing of the non-solubilized material by centrifugation, an equal volume of the same buffer without digitonin (pH 9.0) and either relative CyDye (0.34 mM) or G-Dye (0.41 mM) was added. The labeling lasted for 30 min at 4 °C in the dark. Then, lysine was added and a quenching step was carried out for 10 min at 4 °C. Proteins from the compared variants were pooled and Serva Blue solution was added [37]. Then, 2D BN/Tricine-SDS-PAGE was carried out on 4.5–16% BN and 16.5% Tricine-SDS polyacrylamide gels [83,102]. BioRad Protean II protein gel electrophoresis system employing 20 × 25 cm gels (1.5 mm thick for BN-PAGE, and 1 mm thick for Tricine-SDS-PAGE) or SE 6000 Hoefer system with gel size 18 × 16 cm (1 mm thick for both directions) were used. BN-PAGE was run at 100 V, 15 mA for 45 min and then at 15 mA for 16 h with the voltage limited to 500 V (all steps at 4 °C). Tricine-SDS-PAGE was run for 16 h at 30 mA with the voltage limited to 500 V.

2.7. DIGE image acquisition and analysis, identification of proteins

For Cy2-, Cy3- and Cy5-image acquisition, $\lambda_{ex}/\lambda_{em}$ settings of 488 nm/520 nm, 532 nm/580 nm and 633 nm/670 nm were used, respectively, using a Typhoon TRIO scanner (GE Healthcare). For G-Dye100-, G-Dye200- and G-Dye300-image acquisition, $\lambda_{ex}/\lambda_{em}$ settings of 473 nm/510 nm, 532 nm/575 nm and 635 nm/665 nm were used, respectively, using a FLA-5100 scanner (according to the recommendations of NH DyeAGNOSTICS). Gels were scanned with a 100 μm-pixel size and analyzed using Delta2D (v.4.3.2; DECODON, Germany). A merged image including all gel replicas was assembled. The identification of stress-responsive proteins from the DIGE gels was carried out using the GelMap tool (www.gelmap.de) [80]. The gels were stained with colloidal Coomassie Brilliant Blue (CBB) [64] or with silver nitrate [38]. Protein-containing spots were excised from the gels. After trypsin digestion, the proteins were identified by liquid-chromatography electrospray-ionization-quadrupole time-of-flight mass spectrometry (LC-ESI-Q-TOF-MS) [48] using the MASCOT search algorithm (Matrix Science) against an Arabidopsis protein database (www.Arabidopsis.org; release TAIR 9) and SwissProt and NCBI non-redundant protein databases (www.ncbi.nih.gov).

2.8. Oxygen consumption measurements

Oxygen consumption was measured polarographically using a Clarke-type oxygen electrode (Hansatech Instruments, UK) at 25 °C in 0.5 ml of an incubation medium [72] containing 20 mM HEPES, 350 mM mannitol, 1 mM KH_2PO_4, 5 mM $MgCl_2$ and 0.5% bovine serum albumin (to prevent free fatty acid-induced activity of uncoupling proteins), pH 7.2. All measurements were carried out with 125 μg of mitochondrial proteins in the presence of 10 mM malate (CI-sustained respiration measurements), 10 mM succinate (CII-sustained respiration measurements). Rotenone-insensitive internal NADH dehydrogenase (NDH) activity was measured after malate-sustained respiration was inhibited by rotenone (4 μM) and enhanced by the addition of NAD^+ (1.12 mM). The succinate-sustained respiratory rate measurements were obtained in the presence of rotenone (4 μM), to block the electron transfer from CI, and 0.35 mM ATP to activate succinate dehydrogenase. The phosphorylating (State 3) respiratory rate, the ADP/O ratio and the respiratory control ratio (RCR) were determined with 200 μM ADP. For the ADP/O ratio determination, the total amount of oxygen consumed during State 3 respiration was used. For RCR calculations, the rate of State 3 respiration was divided by the rate of State 4 (non-phosphorylating) respiration following State 3. The cytochrome pathway was inhibited with cyanide (1 mM), and the succinate-sustained AOX activity was first stimulated by 4 mM pyruvate and finally inhibited with 1 mM benzohydroxamate. Because benzohydroxamate completely abolished the cyanide-resistant respiration (no residual oxygen uptake), we attributed this respiration to AOX activity. The maximal activity of CIV was estimated using 125 μg of mitochondrial protein without an exogenously added respiratory substrate and in the presence of sequentially added antimycin A (4 μg mg^{-1} of mitochondrial protein), 8 mM ascorbate, 0.06% cytochrome *c* and up to 0.3 mM *N*,*N*,*N*′,*N*′-tetramethyl-*p*-phenylenediamine (TMPD). The rate of oxygen uptake following the addition of TMPD reflected the maximal oxygen consumption by CIV. Outer mitochondrial membrane integrity was assayed as the latency of CIV activity during the same measurements, i.e., the acceleration of respiration by adding cytochrome *c* prior to the addition of TMPD. The values of oxygen uptake are given in nmol O min^{-1} mg^{-1} of mitochondrial protein.

2.9. In organello protein synthesis

For translation assays (1.5 h at 25 °C), freshly isolated mitochondria (200 μg) were suspended in 100 μl of the synthesis mix [12], and 30 μCi of [^{35}S] methionine (1175 Ci $mmol^{-1}$, Hartmann Analytic) was added. For pulse-chase, the reactions were supplemented with 0.35 ml of synthesis mix containing 10 mM unlabeled methionine and incubated for an additional 5 min at 25 °C. Afterwards, the mitochondria were pelleted, washed and labeled, and the mitochondrial proteins were subjected to 12% SDS-PAGE, electroblotted onto Immobilon-P membranes (Millipore) and autoradiographed. To estimate the relative contribution of the radiolabeled α subunit of mitochondrial ATP synthase (ATP1), cytochrome *c* oxidase subunit 2 (COX2) and the NAD9 subunit of CI in the total labeled protein pool, the signals were quantified with Multi Gauge (v.2.2).

2.10. SDS-PAGE, Western blotting and immunodetection of proteins

Western blotting from SDS polyacrylamide gels was carried out as described by Rurek et al. [81]. Protein Cs resolved by BN-PAGE were reduced first in a solution containing 50 mM Tris–HCl pH 6.8, 1% SDS and 143 mM 2-mercaptoethanol, and then electroblotted in semidry conditions onto Immobilon-P membranes, using a Fastblot B31 semidry blotting apparatus (Biometra). Immunodetection of proteins was carried out with rabbit polyclonal antibodies directed against the α (ATP1, 1:50,000, from G. Schatz, University of Basel) and β (ATP2, 1:1000, Agrisera) subunits of ATP synthase, the NAD9 subunit of CI (1:50,000, [52]), the COX2 subunit of CIV, voltage-dependent anion channel isoform 1 (VDAC1), isocitrate dehydrogenase (IDH), aconitase (ACO) and FtSH4 metalloprotease (all in 1:5000 dilution, Agrisera), and mouse monoclonal antibodies directed against AOX (1:1000, GE Healthcare, [21]), and ATP1 (1:100, [56]). Details of the immunoassays were described previously by Rurek [81]. Enhanced chemiluminescence (ECL) signals were quantified with Multi Gauge (v.2.2).

2.11. RNA isolation, semiquantitative RT-PCR and quantitative (q-RT-PCR) assays

Total RNA from cauliflower curds was extracted using Trizol Reagent (Invitrogen) according to the manufacturer's protocol. Genomic DNA contaminants were removed by RQ1 DNase I free of RNase (Promega). cDNA was synthesized using 1 μg of RNA, 0.2 μg of random hexamers (Fermentas) and 200 units of M-MLV reverse transcriptase (Promega) in a 20-μl total volume for 1 h at 37°C. After first strand synthesis, the reaction mixture was 4 times diluted with 10 mM Tris–HCl, pH 8.0, and, after normalization, aliquots of 1–2 μl were subjected to semiquantitative multiplex RT-PCR in a 15–25 μl total volume or quantitative RT-PCR (q-RT-PCR) using the Thermo Scientific Maxima SYBR Green/ROX qPCR Master Mix kit on an Applied Biosystems 7900HT Fast Real-Time PCR System. Cauliflower cDNA fragments for selected mitochondrial proteins were amplified using specific primers and a 239-bp fragment of cauliflower actin1 (*ACT1*) cDNA was used as an internal standard (Supplementary Table 1). The amplicons were cloned into pGEM-T Easy (Promega) vectors and sequenced bi-directionally (Big Dye Terminator v.3.1 Cycle Sequencing kit, Applied Biosystems) on an ABI Prism 31.30 XL system (Applied Biosystems). Semiquantitative multiplex RT-PCR was performed in an Applied Biosystems 2720 thermal cycler with the following profile: 3 min at 95°C followed by 28 cycles of 20 s at 95°C, 30 s at 55°C (except 44°C and 58°C for *AOX1d* and *cox2*, respectively), and 30 s at 72°C, and with a final incubation for 5 min at 72°C. Amplification of *AOX1b* and *AOX2* cDNAs was conducted with the following profile: 2 min at 98 °C followed by 30 cycles of 20 s at 95°C, 30 s at 53°C, and 45 s at 72°C, and with a final incubation for 10 min at 72°C. The PCR products were separated on a 2% agarose gel and stained with ethidium bromide. The gels were documented using a GBOX XL1.4 (Syngene) imaging system and quantified with Multi Gauge (v.2.2). For the q-RT-PCR analyses, a distinct profile was used: 10 min at 95°C followed by 45 cycles of 20 s at 95°C, and 1 min at 60°C), followed by 15 s at 95°C and 1 min at 60°C, and then a slow temperature increase of 2% per second until 15 s at 95°C. The quality of the q-RT-PCR assays was verified by LinRegPCR (v.2012.3), and the data were analyzed using GenEx (v.5.4.2.128, MultiD Analyses AB, Sweden) software with a manual elimination of outliers. The "two-standard curve" quantification method (each of curves with 6 dilution points of cloned cauliflower *AOX1a* and *ACT1* genomic sequences) was used, and the expression was normalized to the average level (mean log expression equal to 1). Two biological and five technical replicates were included.

2.12. Electron microscopy

The procedure was adapted from Bagniewska-Zadworna et al. [6] with modifications. Small pieces (1 × 1 mm) of the topmost apical layer of cauliflower curds were fixed in 1 ml of fixation solution (2% paraformaldehyde and 2% glutaraldehyde) for 14 h at 4°C, washed with 50 mM sodium cacodylate buffer (pH 7.2), post-fixed in 1% OsO_4, contrasted in 2% uranyl acetate, dehydrated in a step gradient of ethanol and finally embedded in Spurr resin. Ultrathin sections were obtained using Reichert UltracutS and Leica EM UC6 ultramicrotomes, and post-stained for 10 min successively in 5% uranyl citrate and a saturated lead citrate solution for analysis under a transmission electron microscope (TEM) JEM 1200EXII (Jeol). Analysis of the mitochondria number, area occupied by all mitochondria or single mitochondrion in TEM micrograph field images [9] was carried out on field images representing each variant at x7500 direct magnification. Microscopic preparations were made from at least 3 cauliflower curds in 3 independent biological replicates and the representative results were shown. The image analysis was performed using ImageJ 1.43 m.

2.13. Statistical analysis

All experiments were conducted in triplicate, unless otherwise indicated. The respiratory rate values were obtained from five independent experiments (mitochondria preparations) and each determination was performed at least in duplicate throughout the oxygen uptake measurements. The results of the densitometric, microscopic and polarographic analyses (Sections 2.5, 2.8–2.12, 3.5–3.8), and the 2D DIGE spot pattern alterations based on the spot volume (Section 2.7) are presented as the means ± S.E. An unpaired two-tailed Student's *t*-test was used to identify significant differences; in particular, differences were considered to be statistically significant if $p < 0.05$ (*), $p < 0.01$ (**), or $p < 0.001$ (***). Principle component analysis (PCA) was utilized for the assessment of DIGE image quality and reproducibility within the compared variants. The q-RT-PCR data (Section 2.11) was verified with the non-parametric Kolomogorov-Smirnov and Mann-Whitney tests.

3. Results and discussion

3.1. The level of non-respiratory chain complexes is affected by heat stress

Data on the plant mitochondrial complexome in cold and heat stress, especially for stress recovery, are very scarce. Taking into account the results of Tan et al. [88], who postulated the concerted regulation of various mitochondrial proteins in cold exposure, leading to possible changes in Cs abundance, we focused on elucidating alterations in plant mitochondrial Cs under heat and heat recovery. Initially, we inspected the general pattern of respiratory Cs and supercomplexes (SCs) by BN-PAGE. Known respiratory complexes were identified, including SCI+III_2, CI, the ATP synthase holoenzyme, a dimer of complex III ($CIII_2$), CIV and CII (Fig. 1A, *top*). CIV in mitochondria from cauliflower curds appeared to be present in two isoforms (*a* and *b*) detected by standard COX2 antibodies (Fig. 1A, *bottom*), similar to potato stem mitochondria and contrary to potato tuber mitochondria, where only a single active CIV isoform *a* (CIV*a*) is present [23]. No apparent changes in the abundance and stability of the respiratory Cs were observed under stress conditions.

During oxidative stress, matrix Cs may be reassembled and their activity strictly regulated [67]. Because the BN pattern of cauliflower curd mitochondria is dominated by respiratory chain Cs and SCs, we performed Western immonoassays to evaluate the expression levels of the matrix (ACO and IDH) and membrane non-respiratory (VDAC1) complexes (Fig. 1B). Cauliflower mitochondrial ACO (ca. 100 kDa monomers) was present in >700 kDa Cs, which were unstable in heat recovery, and in more stable180–250 kDa Cs. Because the applied ACO1 antibodies (Agrisera) can cross-react with ACO2 and ACO3, it is unclear which of them may be affected by heat in cauliflower. ACO2 and ACO3 are predominantly localized in plant mitochondria [10]. Protein Cs with molecular masses (209 and 144 kDa) similar to those of cauliflower Cs that contain only ACO2 (AT4G26970) are present in Arabidopsis mitochondria [47]. In cauliflower mitochondria (Fig. 1B), IDH (ca. 45 kDa monomers) was mostly present in two heat-stable Cs (ca. 120 and 180 kDa), which were slightly less abundant in heat recovery. VDAC1 (ca. 30 kDa monomers) was present within few Cs of approximately 100, 200 and 400 kDa, and their abundance was also slightly decreased in heat recovery (Fig. 1B). This observation is consistent with a decrease in VDAC level in heat recovery (Section 3.2). Arabidopsis Cs of similar size (i.e., 90–150 kDa for IDH and 100–300 kDa for VDAC1) also contain the mentioned proteins [47].

Because temperature stress may lead to an excessive protein degradation [90], an investigation of the abundance of selected mitochondrial proteases was also warranted. We focused on protein Cs containing FtSH4, a membrane ATP-dependent metalloprotease involved in the degradation of mitochondrial membrane proteins [55]. In cauliflower curd mitochondria, large molecular mass Cs containing FtSH4 (>1.5 MDa and ca. 550 kDa) remained stable in heat but strongly

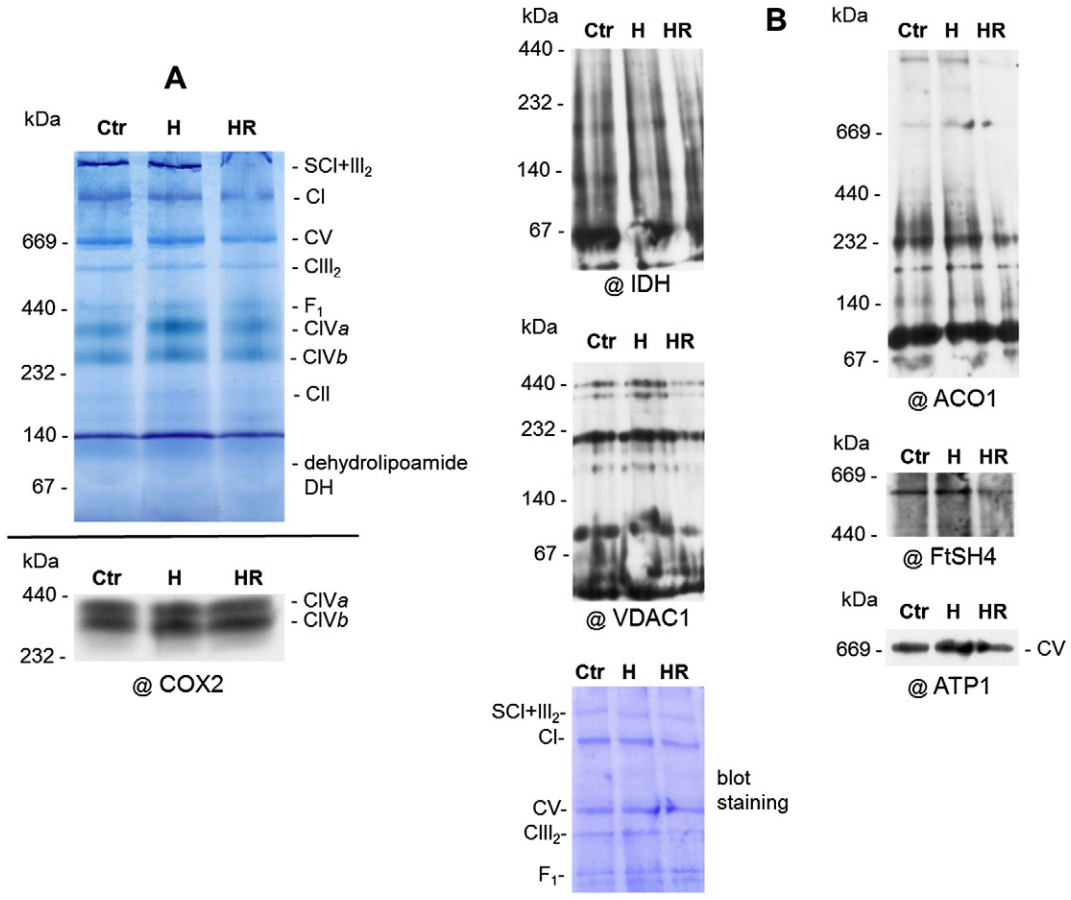

Fig. 1. Analysis of cauliflower mitochondrial complexes during heat stress (H) and heat recovery (HR). (A) Stained BN gel showing the quality of the main respiratory complexes (Cs) and supercomplexes (SCs) solubilized with digitonin (*top*). Two isoforms of CIV were identified on BN blot using immunoassay with antibodies against CIV subunit (@COX2). (B) Western blot analysis of mitochondrial Cs on a representative BN CBB-stained blot using antibodies against all isoforms of aconitase (@ACO1), isocitrate dehydrogenase (@IDH), mitochondrial porin isoform 1 (@VDAC1) and FtSH4 metalloprotease (@FtSH4). For a loading control, the level of subunit-α of mitochondrial ATP synthase was determined using the appropriate antibody (@ATP1). The equal protein loading was also shown by CBB staining of Western blots. Ctr, control. For molecular mass calibration (kDa) of protein Cs, the High Molecular Weight Calibration Kit (Amersham Bioscience) was used.

decreased in abundance after heat recovery (Fig. 1B). These results complement expression data of the *ftsh4* gene for similar stress conditions [86]. Arabidopsis FtSH4 is only present in larger Cs (ca. 1.5 MDa), which are similar in molecular mass to the ones of cauliflower [93]. On the whole, the conventional BN-PAGE allowed us to uncover some alterations, but only in some matrix Cs rather than in respiratory Cs.

DIGE technology allowed for monitoring of the quantitative and qualitative changes in plant proteomes under various stress conditions [2,43,45,46]. In the present study, for the first time, we applied the DIGE approach to elucidate the changes in the plant mitochondrial complexome under heat stress and recovery.

3.2. Heat stress and heat recovery cause a limited destabilization of the cauliflower curd mitochondrial complexome

Experimental variants for DIGE were analyzed in pairs as follows: heat treatment *vs.* control and heat recovery *vs.* control. The minimal labeling of cauliflower mitochondrial Cs was carried out using the CyDye and G-Dye systems. Optimization of the fused image from all CyDye images by spot editing resulted in a final number of 174 spots (Supplementary Fig. 2A, B). The number of spots in the fused G-dye images was slightly higher (up to 454) due to more efficient labeling (Supplementary Fig. 2C). However, the reproducibility of the results obtained with CyDyes with the alternative labeling system (G-Dyes) was limited, most likely due to the different sizes and shapes of fluorescent dyes from various vendors. Because CyDyes are well-recognized in minimal labeling, the results obtained with this system are presented below.

Principle component analysis (PCA) indicated significant differences between the control and treated samples in the image pattern (Supplementary Fig. 2D). The GelMap tool was used to compare the cauliflower and Arabidopsis proteomic maps and identify the affected protein spots. Because, we investigated the mitochondrial proteome from non-green apical part of cauliflower curds, the use of a reference BN/SDS-PAGE map of Arabidopsis cell culture mitochondria was advisable. Interestingly, 9 spots were proposed to contain more than a single protein or protein isoform (Tables 1 and 2).

After heat stress, specifically downregulated spots (not overlapping with the heat-recovery image pattern) were related to translocase of the inner membrane protein (TIM10) and a plant-specific CI subunit (AT1G67785). The upregulated proteins were related to various CI subunits (B14, 51, 75 kDa, also plant-specific AT4G20150) and a precursor of subunit *b* of ATP synthase (Fig. 2, *top*; Table 1). The downregulated spots specific to heat recovery were related to a CIII subunit (QCR8), voltage-dependent anion channel 2 (VDAC2), translocase of the outer membrane subunit (TOM40), the ND7 subunit of CI, malate dehydrogenase 1 (MDH1), ADP/ATP carrier protein 1 and subunit-α of mitochondrial processing peptidase (MPPα). The upregulated spots were TOM9-2, the SDH3 and SDH4 subunits of CII, the QCR9 and 6-1 subunits of CIII and a plant-specific CI subunit (AT4G16450) (Fig. 2, *bottom*; Table 2). Twenty three protein spots overlapped in both the heat and the heat recovery conditions. The downregulated

Table 1
Protein spots up- or downregulated after heat stress in cauliflower mitochondrial complexome. The parameters referred to the quantitative data analyzed by Delta2D were displayed. Mean normalized volumes of indicated spots were calculated from three replicas named after experimental variants (KforH [=CtrH] are controls for heat stress and heat (H) treatment variants). Only spots regulated with at least 1.5- fold change were shown ($p \leq 0.05$). Mean ratios as well as labels related to protein spots up-regulated in heat stress were red-highlighted and those related with down-regulated proteins- highlighted in green. Protein predictions were proposed basing on GelMap data for Arabidopsis cell culture mitochondria (BN/SDS-PAGE) and the relevant reference spot numbers were shown (https://gelmap.de/231) together with proposed accessions of Arabidopsis homologs. Some identifications comprised more than the single protein. n.d., identity not determined. Protein spots regulated both in heat and heat recovery (see also Table 2) were highlighted in gray.

Ratio of mean normalized volume 'H'/ mean normalized volume 'CtrH'	t–Test of mean normalized volume 'H'/ mean normalized volume 'CtrH'	Label	Protein prediction (in square brackets spot label for reference GelMap)	Arabidopsis homolog accession no.	Remarks
−6.20975	0.01341	ID94109	B14.7 (CI subunit) [147]/18 kDa subunit (CI) [147]	AT2G42210/ AT5G67590	2 possible proteins
−4.41845	0.0323	ID94122	QCR7–1 (14kDa; CIII subunit) [20]	AT4G32470	
−2.95462	0.0181	ID94114	n.d.		
−2.57112	0.01524	ID94225	n.d.		
−2.36518	0.02428	ID94125	n.d.		
−2.26031	0.00159	ID94123	QCR7–1 (14kDa; CIII subunit) [54]/QCR7–2 (14 kDa; CIII subunit) [54]	AT4G32470/ AT5G25450	2 possible proteins
−1.78324	0.02315	ID94050	γ subunit (ATP synthase) [64]	AT2G33040	
−1.77349	0.03303	ID94138	n.d.		
−1.75614	0.04178	ID94156	TIM 10 [169]	AT2G29530	
−1.51521	0.0398	ID94221	At1g67785 (plant specific CI subunit) [193]	AT1G67785	
1.53171	0.03067	ID94960	SDH1–1 (succinate dehydrogenase subunit 1–1) [94]	AT5G66760	
1.55595	0.01314	ID94247	QCR10 (CIII subunit) [58]	AT2G40765	
1.6323	0.00189	ID94187	QCR9 (CIII subunit) [56]/QCR6–1, Hinge protein (CIII subunit) [56]	AT3G52730/ AT1G15120	2 possible proteins
1.64834	0.01256	ID93978	75 kDa subunit (CI) [171]	AT5G37510	
1.65297	0.04699	ID94183	At4g20150 (plant specific CI subunit) [160]	AT4G20150	
1.71427	0.01263	ID94004	51 kDa subunit (CI) [172]	AT5G08530	
1.71795	0.0009	ID94133	B14 (CI subunit) [189]/At2g27730 (plant specific CI subunit [152]/At1g67350 (plant specific CI subunit) [151]	AT3G12260/ AT2G27730/ AT1G67350	3 possible proteins
1.72007	0.01753	ID94010	n.d.		
1.72329	0.00958	ID93990	NAD–dependent malic enzyme 2 [59]	AT4G00570	
1.73244	0.00383	ID94193	n.d.		
1.76951	0.02148	ID94128	n.d.		
1.77278	0.00962	ID93989	n.d.		
1.84564	0.00276	ID94165	At4g00585 (plant specific CI subunit) [190]	AT4G00585	
1.85247	0.00549	ID93986	n.d.		
1.86957	0.03689	ID94046	n.d.		
1.90169	0.00024	ID94003	ALDH2 (aldehyde dehydrogenase 2) [79]	AT3G48000	
1.90271	0.01175	ID93987	n.d.		
1.94884	0.00077	ID94178	n.d.		
1.98536	0.00329	ID93998	ALDH5F1 (aldehyde dehydrogenase 5F1) [96]/P5CDH (pyrroline–5–carboxylate dehydrogenase) [96]	AT1G79440/ AT5G62530	2 possible proteins
2.00192	0.00043	ID94104	n.d.		
2.017	0.0445	ID93985	n.d.		
2.065	0.00036	ID94176	ASHI (CI subunit) [158]	AT5G47570	
2.20017	0.00003	ID94186	At4g20150 (plant specific CI subunit) [43]/B12–1 (CI subunit) [43]	AT4G20150/ AT1G14450	2 possible proteins
2.42235	0.03921	ID94159	n.d.		
2.55423	0.04091	ID94006	n.d.		
2.56166	0.03037	ID94065	subunit b (ATP synthase)	ATMG00640	identified also by LC–MS/MS
2.76368	0.00028	ID94045	39 kDa subunit (CI) [142]	AT2G20360	
3.03633	0.00016	ID94041	n.d.		
3.3187	0.04892	ID94042	n.d.		

spots corresponded to the B14.7 and 18-kDa subunits of CI, the QCR7-1 and QCR7-2 subunits of CIII and subunit-γ of ATP synthase. The upregulated spots included CI subunits (ASHI, B12, 39 kDa, AT4G00585; AT4G20150), the SDH1-1 subunit of CII, CIII components (QCR6, QCR9 and QCR10), aldehyde dehydrogenase (ALDH2B4 and 5 F1), pyrroline-5-carboxylate dehydrogenase (P5CDH) and malic enzyme (Tables 1 and 2).

Overall, we noticed prevalent upregulation in the mitochondrial complexome after heat treatment and more specific alternations after heat recovery, likely representing adaptations in the subunit content

Table 2
Protein spots up- or downregulated after heat recovery in cauliflower mitochondrial complexome. The parameters referred to the quantitative data analyzed by Delta2D were displayed. Mean normalized volumes of indicated spots were calculated from three replicas named after experimental variants (K [= CtrHR] are controls and heat recovery (HR) variants). Only spots regulated with at least 1.5-fold change were shown ($p \leq 0.05$). Mean ratios as well as labels related to protein spots up-regulated in heat recovery were red-highlighted and those related with down-regulated proteins were highlighted in green. Protein predictions were proposed basing on GelMap data for Arabidopsis cell culture mitochondria (BN/ SDS-PAGE) and the relevant reference spot numbers were shown (https://gelmap.de/231) together with proposed accessions of Arabidopsis homologs. Some identifications comprised more than the single protein. n.d., identity not determined. Protein spots regulated both in heat (see also Table 1) and heat recovery were highlighted in gray.

Ratio of mean normalized volume 'HR' / mean normalized volume 'CtrHR'	t–Test of mean normalized volume 'HR' / mean normalized volume 'CtrHR'	Label	Protein prediction (in square brackets spot label for reference GelMap)	Arabidopsis homolog accession no.	Remarks
−13.54536	0.0001	ID94109	B14.7 (CI subunit) [147]/18 kDa subunit (CI) [147]	AT2G42210/ AT5G67590	2 possible proteins
−4.4448	0.00479	ID94122	QCR7–1 (14kDa; CIII subunit) [20]	AT4G32470	
−3.27502	0.00492	ID94114	n.d.		
−2.81695	0.00005	ID94050	γ subunit (ATP synthase) [64]	AT2G33040	
−2.34534	0.00267	ID94057	γ subunit (ATP synthase) [33]	AT2G33040	
−2.33494	0.03551	ID94224	QCR8 (Isoforms: At3g10860, At5g05370; CIII subunit) [25]	AT3G10860, AT5G05370	2 possible isoforms
−2.30061	0.04299	ID94016	n.d.		
−2.0673	0.00012	ID94123	QCR7–1 (14kDa; CIII subunit) [54]/QCR7–2 (14 kDa; CIII subunit) [54]	AT4G32470/ AT5G25450	2 possible proteins
−1.91811	0.00481	ID94052	VDAC2 (voltage dependent anion channel 2) [83]	AT5G67500	
−1.81959	0.02873	ID94023	TOM40 [63]	AT3G20000	
−1.80055	0.00035	ID94138	n.d.		
−1.74659	0.01633	ID94024	ND7 (CI subunit) [141]	ATMG00510	
−1.5962	0.00396	ID94870	malate dehydrogenase 1 [131]/AAC1 (ADP/ATP carrier 1) [131]	AT1G53240/ AT3G08580	2 possible proteins
−1.57894	0.04707	ID94009	MPPα–1 (CIII) [3]	AT1G51980	
1.50878	0.03128	ID94128	n.d.		
1.62731	0.00334	ID94182	TOM9–2 [195]	AT5G43970	
1.63415	0.00058	ID94203	SDH4 (succinate dehydrogenase subunit 4) [91]	AT2G46505	
1.6353	0.02476	ID94097	n.d.		
1.71791	0.00132	ID94174	QCR9 (CIII subunit) [55]/QCR6–1, Hinge protein (CIII subunit) [55]	AT3G52730/ AT1G15120	2 possible proteins
1.74863	0.00012	ID94187	QCR9 (CIII subunit) [56]/QCR6–1, Hinge protein (CIII subunit) [56]	AT3G52730/ AT1G15120	2 possible proteins
1.77777	0.00874	ID94186	At4g20150 (plant specific CI subunit)/B12–1 (CI subunit) [43]	AT4G20150/ AT1G14450	2 possible proteins
1.80818	0.03113	ID94045	39 kDa subunit (CI) [142]	AT2G20360	
1.83249	0.03453	ID93998	ALDH5F1 (aldehyde dehydrogenase 5F1) [96]/P5CDH(pyrroline–5–carboxylate dehydrogenase) [96]	AT1G79440/ AT5G62530	2 possible proteins
1.86411	0.03447	ID94960	SDH1–1 (succinate dehydrogenase subunit 1–1) [94]		
1.94852	0.0282	ID94193	n.d.		
1.99019	0.01333	ID93979	n.d.		
2.03347	0.01628	ID94003	ALDH2 (aldehyde dehydrogenase 2) [79]	AT3G48000	
2.03622	0.00068	ID94171	At4g16450 (plant specific CI subunit) [192]	AT4G16450	
2.13894	0.00292	ID94176	ASHI (CI subunit) [158]	AT5G47570	
2.23356	0.00175	ID94247	QCR10 (CIII subunit) [58]	AT2G40765	
2.25058	0.00041	ID94165	At4g00585 (plant specific CI subunit) [190]	AT4G00585	
2.55413	0.0003	ID93986	n.d.		
2.59748	0.02226	ID93992	n.d.		
2.61947	0.03298	ID94042	n.d.		
2.7322	0.01419	ID93985	n.d.		
2. 77087	0.00064	ID93987	n.d.		
2.83328	0.01562	ID93990	NAD–dependent malic enzyme 2 [59]	AT4G00570	
2.88268	0.00772	ID94146	SDH3–2 (succinate dehydrogenase subunit 3–2) [113]	AT4G32210	
2.95729	0.00637	ID94041	n.d.		
3.06805	0.03066	ID94007	n.d.		
3.3178	0.0317	ID94006	n.d.		

of protein Cs (Tables 1 and 2). Some changes occurred in enzymes of primary carbon or amino acid metabolism and components of the import machinery, and the mitochondrial transporter system. Although we noticed numerous changes in the abundance of specific subunits of respiratory Cs, we were not able to find concerted regulation of subunits between various Cs, including reciprocal alterations in subunit levels

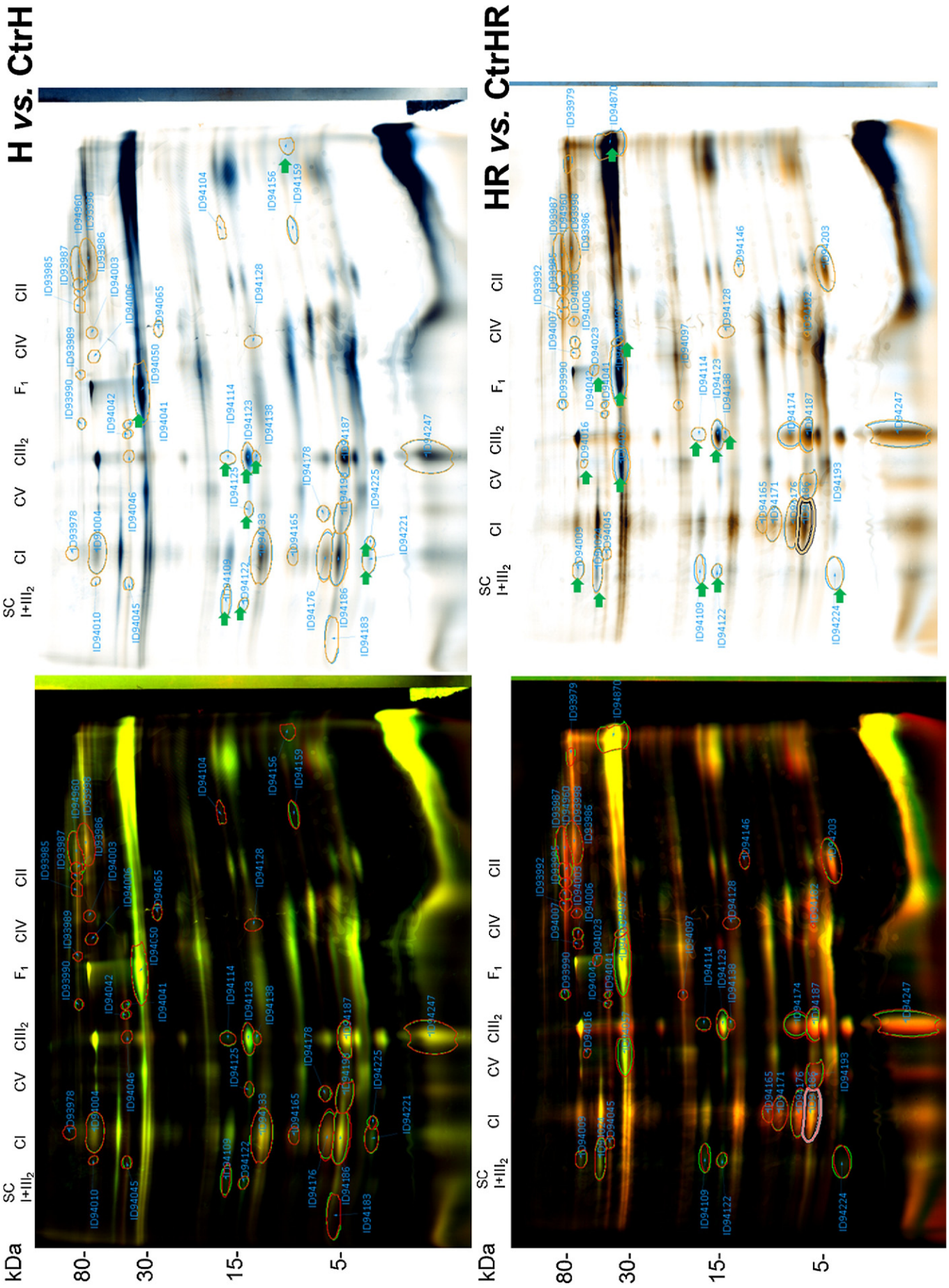
H vs. CtrH
HR vs. CtrHR
kDa
80-
30-
15-
5-
SC I+III2
CI
CV
CIII2
F1
CIV
CII

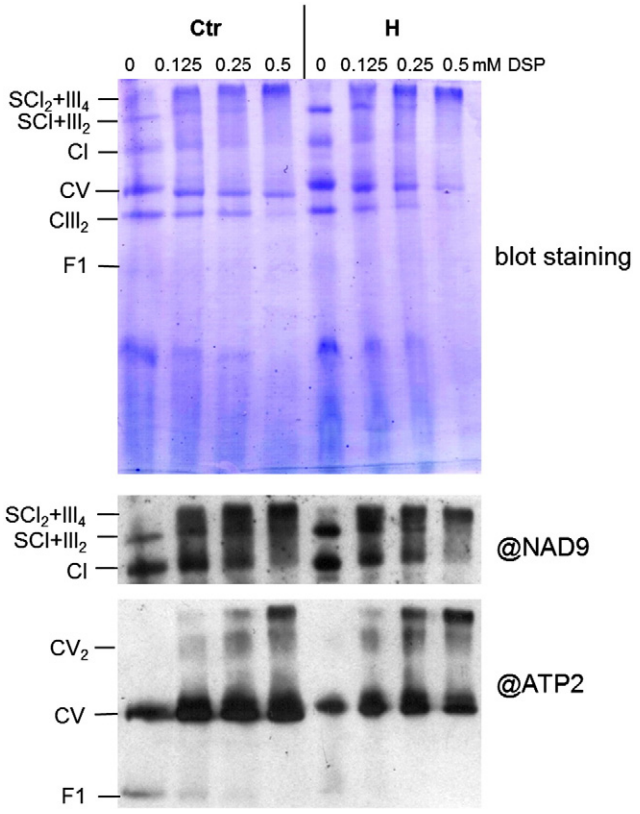

Fig. 3. Chemical crosslinking of respiratory Cs during heat stress. Cauliflower mitochondrial Cs and SCs from control plants (Ctr) and plants subjected to heat stress (H) were DSP-crosslinked, solubilized with digitonin and assayed by BN-PAGE. The proteins are indicated on a CBB-stained Western blot. Immunodetection of the NAD9 subunit of CI and subunit-β of ATP synthase was conducted with respective antibodies (@NAD9 and @ATP2). For molecular mass calibration (kDa) of protein Cs, the High Molecular Weight Calibration Kit (Amersham Bioscience) was used.

between SCI+III_2 and free Cs. The exceptions were the ID94183/ID94186 and ID94122/ID94123 spots for the SCI+III_2/CI and SCI+III_2/CIII subunits, respectively (Fig. 2). The decreased ratio of spot fluorescence intensity between treated and control variants may suggest a dissociation of the subunit from the complex and its subsequent destabilization. Downregulation of the subunit amount would affect the level and size of the Cs and lead to their subsequent faster migration during BN-PAGE, which was not the case. All these observations led us to the intriguing conclusion that despite previous assays [37], plant mitochondria may have a relatively stable oxidative phosphorylation (OXPHOS) architecture during temperature stress. However, the resolution capacity of BN gels for large protein Cs has been questioned [58]. Therefore, the possible alterations in stability of respiratory SCs and Cs could not be easily detected.

Reports of putative complexomic alterations induced by abiotic stress treatments are scarce, elevating the relevance of our study. For instance, Lenaz and Genova [54] suggested that harsh oxidative stress results in significant SC disassembly, and Ramírez-Aguilar et al. [75] noted that the stability and activity of potato (*Solanum tuberosum*) large mitochondrial SCs (containing CI, CIII and CIV at diverse stoichiometry) is altered under prolonged hypoxia. Overall, we detected a greater number of regulated respiratory chain components than Obata et al. [67] and Tan et al. [88], who suggested the changed abundance of some mitochondrial Cs. Contrary to our study, Tan et al. [88] has been able to show only downregulations in cold stress using the *gel-free* approach. Only two cauliflower mitochondrial proteins, the B14.7 subunit of CI and ATP synthase subunit-d (Tables 1 and 2), overlapped with the cold-regulated proteins from Tan et al. [88], indicating distinct responses to high temperatures compared to cold treatment in the abundance of plant mitochondrial OXPHOS components. Other proteins we investigated, including ATP synthase subunit-γ, the 75-kDa CI subunit and MDH, are also regulated by cold [19,25,90,103], however, often in the opposite direction from that indicated by our data, which reflects species-specific regulations in plant mitochondrial proteome. Notably, for the first time, some cauliflower CI and CIII subunits with addition to some TIM/TOM proteins were shown (Tables 1 and 2) to be implicated in temperature treatments.

3.3. Cauliflower CII and ATP synthase

We used LC-MS/MS to directly identify seven protein spots (for the CII and ATP synthase subunits), which were collected from silver-stained DIGE gels containing proteins pooled from control and heat-recovered plants (Supplementary Fig. 3). Four CII subunits (SDH1-SDH4) are recognized as universal among all organisms, and another four proteins (SDH5-SDH8) are plant-specific [41]. Recently, variations in subunit content, homology and expression level have been reported for CII in both Arabidopsis and rice (*Oryza sativa*). Because some cauliflower CII subunits (including SDH4) were upregulated mainly after heat recovery, we compared data from cauliflower and Arabidopsis [59]. We concluded that spot no. 3 may represent an additional cauliflower-specific SDH6 isoform, which is in close proximity to the main SDH6 spot. Alternatively, it may represent an uncharacterized protein co-migrating with CII on BN gels (Supplementary Fig. 3). Dicot plants have CII with a similar pattern on BN/SDS-PAGE gels [24]. Notwithstanding, differences in CII subunit content may exist between species belonging to the same family, such as cauliflower and Arabidopsis. Spots 7 (ID94065) and 6 (Supplementary Fig. 3, *bottom*) contained ATP synthase subunit-b, which is homologous to the product of the Arabidopsis mitochondrial *open reading frame25* (*orf25*) gene [36], and the *atpF* gene of *Pseudomonas fluorescens*. Strikingly, the b-subunit of F_O was not assembled into the ATP synthase holocomplex after heat recovery. Together with the downregulation of F_1 subunit-γ (ID94050), this finding suggests perturbations in the biogenesis of the enzyme after stress recovery. In isolated mitochondria, ATP synthase is thermosensitive [37]. The assembly of ATP synthase may be affected as cellular energy demands rise, and the upregulation of ATP synthase subunits may be related to stress response regulation and stress adaptation [34,61]. For instance, overexpression of the ATP6 protein in transgenic Arabidopsis cell suspensions improves the cold resistance [107]. Moreover, the abundance of ATP synthase can be downregulated, for instance, by silencing the Arabidopsis gene encoding for a particular subunit [26].

Despite the overall stability of the OXPHOS architecture, the flexibility of the content of the Cs during temperature stress may play a biological role in cauliflower mitochondria. Interestingly, all detected cauliflower heat stress-responsive CII subunits (Supplementary Fig. 3) did not belong to the accessory proteins that may be variably expressed among plant species [41], which highlights dynamic stress response of plant CII. The balance between CII and CI levels is organ-specific in Arabidopsis. Because the CII levels are elevated in non-green Arabidopsis tissues [70], relatively higher amounts of CII may exist in the apical parts of cauliflower curd (non-green ones) compared with

Fig. 2 A representative 2D-DIGE comparison of cauliflower curd mitochondria from plants subjected to heat stress and heat recovery. The pooled samples applied to DIGE were as follows: heat stress (H) *vs.* respective control (CtrH) and heat recovery (HR) *vs.* respective control (CtrHR). Images are shown in RGY-mode. The labeled spots are mitochondrial proteins, which displayed significant differences in abundance (>1.5-fold change) between treatment and control conditions ($p < 0.05$). The protein molecular mass is indicated in kDa. Left, Cy2-labeled proteins from control (green) are overlaid against Cy3 or Cy5-labeled proteins from H or HR, respectively (red). Right, Cy2-labeled proteins (blue) are overlaid against Cy3- or Cy5-labeled proteins (orange). Downregulated protein spots are indicated by green arrows. Additional data can be viewed in Supplementary Fig. 2 and Tables 1 and 2.

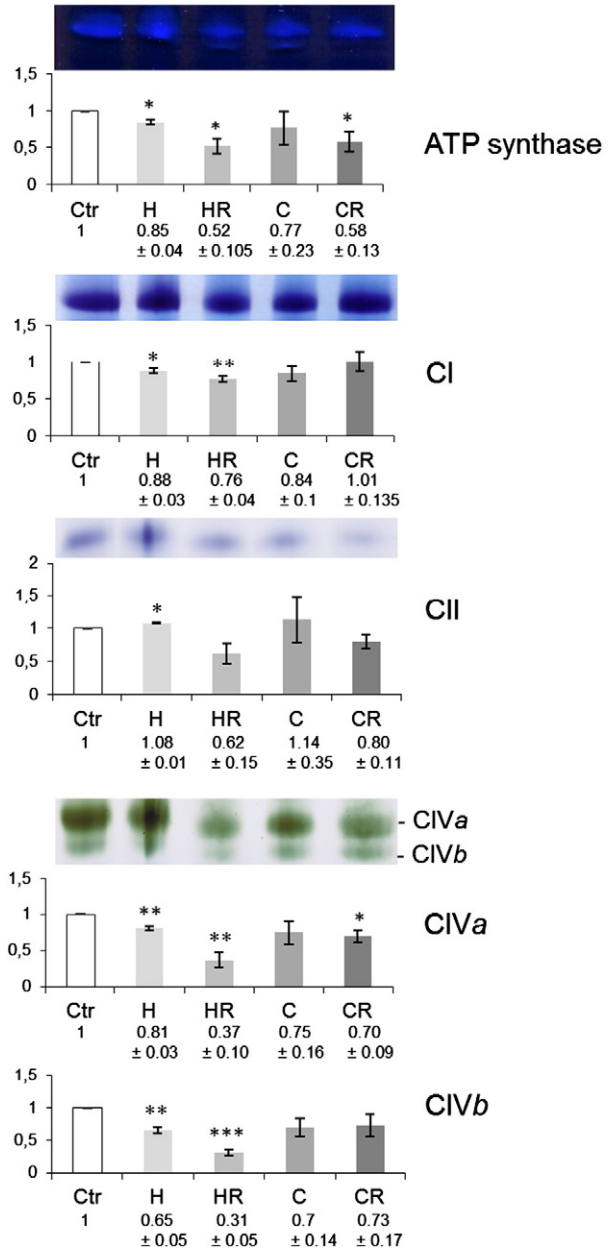

Fig. 4. *In-gel* activity of respiratory Cs under temperature stress conditions. The activity (presented in relative units) was determined for all temperature treatments. Mean values (± S.E.) from triplicates (below graphs) were standardized to the control value (set to 1.00). The data are presented as the means ± S.E. ($n = 3$). ***, $p < 0.001$, **, $p < 0.01$, *, $p < 0.05$ versus control values. Above each graph, representative BN zymograms are shown. Ctr, control; H, heat stress; HR, heat recovery; C, cold treatment; CR, cold recovery.

other organs. Overall, the functional implications of the observed stress-affected structural changes within the OXPHOS components require further exploration.

3.4. Heat stress does not alter the pattern of transient interactions between CI and CIII or between ATP synthase monomers

In order to extend our study to the analysis of interactions between CI and CIII (leading to the formation of $SCI+III_2$ and SCI_2+III_4) and between ATP synthase monomers, we crosslinked mitochondrial extracts with DSP, a membrane-permeable crosslinking agent that is widely used to study protein-protein interactions [49]. Notably, crosslinking has not been used for the analysis of interactions within plant mitochondrial Cs under stress conditions, but mostly to investigate the subunit content and structure of particular Cs [5,98].

Freshly isolated cauliflower mitochondria from control and heat-stressed plants were crosslinked with various concentrations of DSP before being solubilized with digitonin. Afterwards, Cs were resolved by BN-PAGE, electroblotted onto Immobilon-P and probed with antibodies against the NAD9 subunit of CI and the ATP2 subunit of ATP synthase (Fig. 3). The formation of $SCI+III_2$ and its dimerization, leading to the appearance of SCI_2+III_4, and the efficiency of dimerization of mitochondrial ATP synthase (CV_2) were unaffected in mitochondria from heat-treated cauliflower plants (Fig. 3, *bottom*). Strikingly, ATP synthase dimers have been only observed in mitochondria from some plant species [13,24,50]. Moreover, in some species, the mitochondrial ATP synthase dimmer remains more stable under environmental conditions than its plastid counterpart [85].

Our findings are consistent with a significant resistance to structural destabilization due to heat stress in cauliflower respiratory SCs and Cs, as shown by BN-PAGE (Fig. 1A, *top*). Next, we used functional assays to determine what changes in the enzymatic activity of respiratory Cs accompanied the observed proteomic alterations. First, we performed *in-gel* assays for CI, CII, CIV and ATP synthase activity.

3.5. The in-gel activity of respiratory Cs is affected by temperature stress conditions, especially by stress recovery

Recently, Peters et al. [70] reported that CI and CIV are more active in generative organs. Therefore, we were interested in mitochondria from

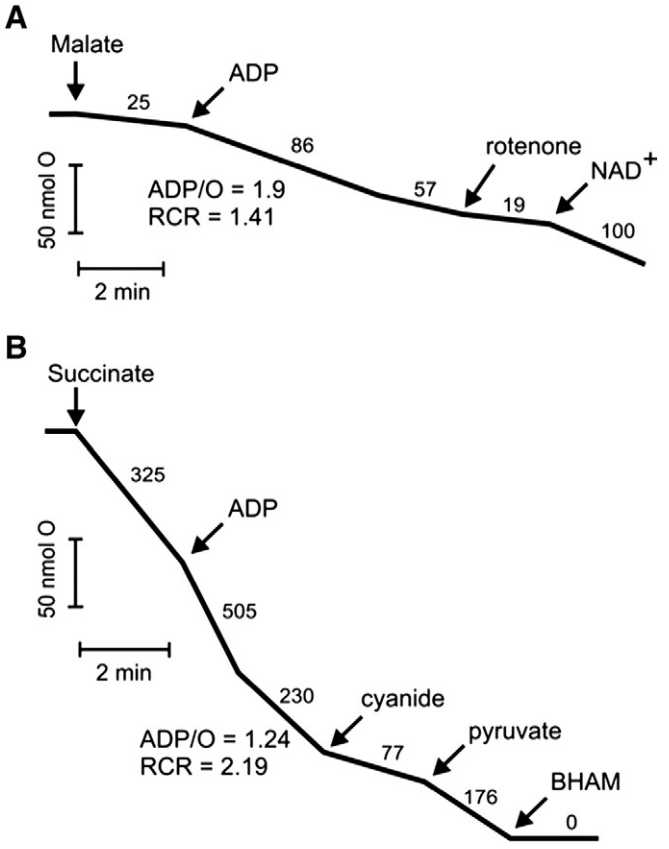

Fig. 5. Determination of mitochondrial respiration in mitochondria isolated from cauliflower curds. The results obtained for mitochondria isolated from heat-stressed plants are shown as an example. Traces representative of ten measurements (using mitochondria from five different preparations) are shown. Respiratory traces with malate (A) and succinate (B) as respiratory substrates are presented. Additions: 10 mM malate, 200 μM ADP, 4 μM rotenone, 1.12 mM NAD^+, 10 mM succinate, 1 mM cyanide, 4 mM pyruvate and 1 mM benzohydroxamate (BHAM) are described in Section 2.8. Numbers on the traces refer to the rates of O_2 uptake and are given in nmol O min^{-1} mg^{-1} of mitochondrial protein.

Table 3
Respiratory rates, coupling parameters and the rotenone-insensitive internal NADH dehydrogenase (NDH) activity of mitochondria isolated from cauliflower curds after exposure to heat stress (H), heat recovery (HR), cold stress (C) and cold recovery (CR). Malate was used as a respiratory substrate. The rates (in nmol O min^{-1} mg^{-1} of mitochondrial protein) of State 4 (non-phosphorylating respiration), State 3 (phosphorylating respiration) and State 4′ (State 4 following State 3) are presented. The assay conditions were as described in Section 2.8. The values of oxygen uptake are given in nmol O min^{-1} mg^{-1} of mitochondrial protein. Mean values (± S.E.) for five different mitochondria preparations of each type (with duplicate measurements, $n = 10$) are shown. Ctr, control; RCR, respiratory control ratio.

Malate-sustained respiration		Ctr	H	HR	C	CR
State 4		39.8 ± 4.5	24.2 ± 2.0*	27.1 ± 1.7*	29.1 ± 3.2*	42.5 ± 3.9
State 3		145 ± 13	84.9 ± 7.6*	82.9 ± 8.2*	136 ± 10	159 ± 12
State 4′		90.2 ± 6.2	58.2 ± 4.0*	59.6 ± 3.4*	74.4 ± 8.3	85.4 ± 3.7
RCR		1.61 ± 0.18	1.46 ± 0.14*	1.39 ± 0.12*	1.83 ± 0.13	1.86 ± 0.17
ADP/O		2.10 ± 0.14	1.86 ± 0.14*	2.21 ± 0.19	2.54 ± 0.15**	2.41 ± 0.20**
Rotenone-insensitive respiration (internal NDH activity)	− NAD^+	27.6 ± 3.4	18.9 ± 1.7**	20.1 ± 2.1*	29.4 ± 2	29.9 ± 3.6
	+ NAD^+	133 ± 24	101 ± 15*	102 ± 18*	126 ± 16	100 ± 14*

** $p < 0.01$.
* $p < 0.05$ versus control values.

cauliflower curds containing inflorescence buds, because altered respiratory Cs activity may be involved in the stress response of respiratory metabolism during the transition from the vegetative stage to the generative stage.

The *in-gel* activities of CI, CII, CIV (two isoforms, *a* and *b*) and ATP synthase were investigated. NADH dehydrogenase activity is present in bands for CI, SCs ($SCI+III_2$ and SCI_2+III_4) and in the dehydrolipoamide dehydrogenase band [57]. In general, in cauliflower curd mitochondria, the activities of most of the investigated respiratory Cs and ATP synthase decreased after heat treatment and heat recovery (Fig. 4). Under heat recovery conditions, this common decrease in activity was more pronounced. In addition, ATP synthase activity and CIV*a* (contrary to CIV*b*) activity decreased after cold acclimation. The *in-gel* activity profile of CIV*a* during temperature stress was similar to that of CIV*b*; however, CIV*a* appeared to be more active than CIV*b*. Thus cauliflower CIV isoforms responded almost in parallel to the stress conditions. We concluded that the impact of heat, especially heat recovery, resulted in a significantly lowered enzymatic activity in respiratory Cs and ATP synthase, which is in line with the majority of the cauliflower mitochondrial proteome alternations detected by 2D DIGE (Tables 1 and 2). The structural destabilization of the Cs or regulation of their subunit levels during abiotic stress (including thermal treatments) may thus be accompanied by changes in their activity. This phenomenon has been observed for potato (*Solanum tuberosum*) mitochondrial SCs and Cs in response to hypoxia; however, these changes reverted after recovery [75].

Afterwards, we elucidated whether *in-gel* activity alterations are reflected at the mitochondrial respiration level by measuring the cytochrome pathway- and alternative pathway-mediated respiration of isolated cauliflower curd mitochondria.

3.6. Basic energetic parameters and alternative respiratory pathways of cauliflower curd mitochondria are differentially affected by temperature stress conditions

Alternative oxidase is regarded as an active modulator of the mitochondrial stress response in plant cells [96]. By measuring oxygen consumption, we determined activities of the cytochrome and alternative pathways using malate and succinate as respiratory substrates in mitochondria isolated from cauliflower plants treated with cold, heat or stress recovery (Fig. 5, Tables 3 and 4). The relative activity of cyanide-resistant AOX-sustained respiration was studied with succinate (Table 4). Moreover, the effect of pyruvate, a strong positive effector of plant AOX and the simplest α-keto acid [15], was studied. In turn, with malate as a respiratory substrate, the capacity of another alternative component of the plant respiratory chain, rotenone-insensitive internal NADH dehydrogenase, was determined (Fig. 5, Table 3).

For all investigated stress and recovery conditions, much higher rates of non-phosphorylating respiration (State 4) and phosphorylating respiration (State 3) were observed with succinate compared to malate (Fig. 5, Tables 3 and 4). This difference between substrates was the most pronounced in heat (even 13 times higher State 4 and almost 6 times higher State 3). However, regardless of the substrate used, a simultaneous statistically significant decrease of both coupling parameters, i.e., the ADP/O and RCR ratios, was detected only after heat treatment (Tables 3 and 4). Because the *in-gel* activity studies (Section 3.5) also

Table 4
Respiratory rates, coupling parameters and the AOX and CIV activities of mitochondria isolated from cauliflower curds after heat stress (H), heat recovery (HR), cold stress (C) and cold recovery (CR). Succinate (plus rotenone) was used as a respiratory substrate. Rates of State 4 (non-phosphorylating respiration), State 3 (phosphorylating respiration), and State 4′ (State 4 following State 3) are presented. Assay conditions were as described in Section 2.8. The values of oxygen uptake are given in nmol O min^{-1} mg^{-1} of mitochondrial protein. The values of outer mitochondrial membrane (OMM) integrity are given in %. Mean values (± S.E.) for five different mitochondria preparations of each type (with duplicate measurements, $n = 10$) are shown. Ctr, control; RCR, respiratory control ratio.

Succinate-sustained respiration		Ctr	H	HR	C	CR
State 4		344 ± 32	322 ± 32	260 ± 24*	206 ± 22**	371 ± 38
State 3		608 ± 46	493 ± 34*	405 ± 42*	381 ± 19**	704 ± 37
State 4′		238 ± 25	228 ± 29	158 ± 17*	147 ± 13**	235 ± 25
RCR		2.56 ± 0.20	2.16 ± 0.15*	2.56 ± 0.21	2.60 ± 0.25	3.00 ± 0.34
ADP/O		1.36 ± 0.09	1.23 ± 0.09*	1.38 ± 0.11	1.41 ± 0.12	1.44 ± 0.09
Cyanide-resistant respiration (AOX activity)	− PA	45.5 ± 4.4	76.9 ± 5.2*	37.5 ± 2.6	24.5 ± 2.6**	51.9 ± 4.4
	+ PA	96.5 ± 9.4	172 ± 11.2*	83.5 ± 5.8	60.6 ± 6.3**	109 ± 8.3
	+ BHAM	0	0	0	0	0
TMPD/ascorbate-sustained respiration (maximal CIV activity)		642 ± 61	471 ± 38**	510 ± 51*	565 ± 63*	598 ± 53
OMM integrity		96.5 ± 0.8%	93.5 ± 0.9%	95.4 ± 0.9%	95.0 ± 0.8%	95.4 ± 1.1%

** $p < 0.01$.
* $p < 0.05$ versus control values.

revealed reduced ATP synthase activity after heat treatment, it indicates that the sensitivity of the OXPHOS system to elevated temperature led to a lowered yield of ATP synthesis. However, our proteome analysis (Section 3.2) suggests that these changes are not accompanied by major structural alterations.

Regardless of the respiratory substrate used, the coupling parameters were comparable after cold recovery compared to mitochondria from cold-treated curds (Tables 3 and 4). However, with succinate, the cold recovery conditions caused a significant increase in State 4 and State 3 respiration compared to cold stress conditions. In turn, after heat stress, heat recovery and cold stress, State 4 and State 3 respiration decreased compared to control mitochondria. These decreased respiratory rates could be the result of a significantly reduced activity of the respiratory Cs, i.e., CI, CII and/or the cytochrome pathway Cs (CIII and/or CIV). Measuring the maximal respiratory activity of CIV in isolated mitochondria (Table 4) revealed that CIV activity was significantly decreased in the heat, heat recovery and cold (compared to control mitochondria). In contrast, cold recovery restored CIV activity to the control value. In general, the changes in the CIV activity in isolated mitochondria (Table 4) closely followed the changes in isoforms of CIV (*a* and *b*) observed in the *in-gel* studies (Fig. 4). Cauliflower CIV activity is much more sensitive to heat stress (including heat recovery) than to cold (including cold recovery). The limitation of the activity of CIV (and the whole ubiquinol-oxidizing cytochrome pathway) may influence the activity of CI and CII (thus the ubiquinone-reducing part of the respiratory chain) and *vice versa*.

After heat recovery, State 3 respiration remained lowered for both respiratory substrates and the ADP/O ratios were significantly increased compared to those during heat (Tables 3 and 4), thus we assume that the yield of ATP synthesis was restored due to the reduced activity of energy-dissipating pathways rather than changes in ATP synthase activity itself (no improvement in State 3 respiration). Thus, during heat recovery, in a relatively short time, the OXPHOS yield was restored. On the other hand, cold recovery did not influence the OXPHOS yield (ADP/O ratios) compared to cold conditions.

The results of the *in-gel* activity studies (Section 3.5) together with mitochondrial respiration measurements (Tables 3 and 4) indicate that: (i) heat stress negatively affects ATP synthase, CI and CIV, but not CII; (ii) heat recovery negatively affects CI, CII and CIV; (iii) cold stress negatively affects CII and CIV, but not CI; and (iv) cold recovery recovers the CI, CII and CIV activities close to those of control conditions. However, some results of the *in-gel* activity (Section 3.5) and oxygen consumption (Tables 3 and 4) studies do not match together. These discrepancies could reflect the impact of the inner mitochondrial membrane on the organization, stability and activity of respiratory chain SCs, which is eliminated during the *in-gel* activity assays [71,106].

Measurements of mitochondrial respiration indicate that rotenone-resistant internal NADH dehydrogenase (NDH) is not a heat stress-induced protein in cauliflower curd mitochondria (Table 3). After heat stress and heat recovery, we noticed a significantly decreased (more than 23% compared to control conditions) unstimulated and NAD^+-stimulated activity of this pathway. Interestingly, a similar decrease in the activity of NDH-mediated respiration was observed for cold recovery, while cold did not change this respiration. Thus, any increase in temperature, i.e., the transition from control temperature to heat and the transition from cold to cold recovery, results in the decrease of NDH-mediated respiration in cauliflower curd mitochondria.

Some functions of AOX in temperature stress have been previously discussed [39]. Grabelnych et al. [30] have noticed that cyanide-resistant AOX-mediated respiration is elevated preferentially in cereal mitochondria under cold, which was in contrast to our study. Namely, the highest AOX activity was observed after heat treatment (Table 4). Heat stress increased the unstimulated AOX activity by 69% and pyruvate-stimulated AOX activity (i.e., AOX capacity) by 78%. Moreover, an increase in temperature during the transition from cold to cold recovery was also accompanied by an increase in unstimulated and pyruvate-stimulated AOX activity. Thus, in cauliflower mitochondria, AOX seems to be a heat-induced protein. Interestingly, heat recovered mitochondria exhibited a decrease in AOX activity compared to heat stress. These results account for the changes in OXPHOS yield (ADP/O ratio) observed in mitochondria isolated after heat stress and heat recovery (Tables 3 and 4). In the heat-treated plants, an increase in the activity of AOX was accompanied by decreases of coupling parameters (for both respiratory substrates). Conversely, the heat recovery restored the coupling parameters to the values observed in control mitochondria. On the other hand, the decrease in AOX activity observed for cold conditions (compared to control conditions) could explain an increase in the coupling parameters (especially the ADP/O ratio) when malate was used as a respiratory substrate. As opposed to heat recovery, cold recovery enhanced AOX activity (compared to cold) that was similar to the control values (Table 4). Thus, it is tempting to conclude that conversely to NDH-mediated respiration (Table 3), any increase of temperature, i.e., the transition from control to heat stress conditions and the transition from cold to cold recovery, promotes an increase in AOX activity in cauliflower curd mitochondria (Table 4). The results obtained with mitochondria isolated from soybean cotyledons [4] support this conclusion. These mitochondria exhibited an increase in pyruvate-stimulated AOX activity with increasing temperatures of the incubation medium.

Despite the clear differences between the AOX activities in mitochondria under all temperature stress conditions, pyruvate exerted a comparable stimulatory effect (a 2.1–2.4-fold increase in AOX activity) in all of the conditions. According to Popov et al. [72], cold treatment increases the cyanide-resistant respiration of bell pepper (*Capsicum annuum*) mitochondria, contrary to cold-treated cauliflower mitochondria. Unlike our study, in Popov's approach, the stress conditions were applied to already-harvested plant organs. However, both approaches for cauliflower curd treatment revealed that AOX is not a cold stress-induced protein in cauliflower mitochondria. In both cases, the AOX activity significantly decreased after cold treatment. A strong co-expression of some AOX and NDH isoforms has been documented [16,76,94]. However, the activities of cauliflower AOX and NDH changed in opposite directions with temperature stress (Tables 3 and 4). Notwithstanding, the co-expression of specific AOX and NDH isoforms may not always occur [16,76].

To link the functional and molecular data, we additionally characterized the stress regulation of AOX at the proteomic and transcriptomic levels. Standard monoclonal antibodies raised against the *Sauromatum guttatum* enzyme cross-reacted with three polypeptides of 29 kDa, 33 kDa and 36 kDa in cauliflower mitochondria, which represent AOX

Fig. 6 AOX abundance at the protein and transcript levels under temperature stress conditions. (A) Analysis of immunoreactive polypeptides (*a*, *b*, *c*) of AOX on representative SDS-PAGE blots using respective antibodies (@AOX). For the loading control, an antibody against subunit-α of mitochondrial ATP synthase (@ATP1) was used. Equal protein loading was also shown by CBB staining of Western blots. For protein size calibration, the PageRuler Prestained Protein Ladder (Thermo Scientific) was used. Protein molecular mass is indicated in kDa. (B) Semi-q-RT-PCR analysis of the relative level of cauliflower *AOX1a*, *AOX1b*, *AOX1d* and *AOX2* transcripts. For normalization, cauliflower actin1 (*ACT1*) was used. Representative 2% agarose gels are shown. *Bottom*: the expected size of cauliflower *AOX1b*, *AOX2* and *ACT1* cDNA amplicons on gel images was indicated with small circles. The size of respective genomic (gDNA) amplicons as positive PCR controls was indicated with small squares. The results of the densitometric analysis in (A) and (B) are presented as the mean values (± S.E.) from triplicate detection. These values were standardized relative to the control (set to 1.00). (C) The relative expression of *AOX1a* determined by q-RT-PCR. Upper graph, expression was normalized to the average level (mean log expression = 1). Bottom graph, differences in $\log_2$ scale between treated and control variants are shown. For normalization, *ACT1* was used. Further data are given in the text. Ctr, control; CtrH, control for heat treatment; CtrC, control for cold treatment; C, cold stress; H, heat stress; CR, cold recovery; HR, heat recovery. ***, $p < 0.001$, **, $p < 0.01$, *, $p < 0.05$ versus control values.

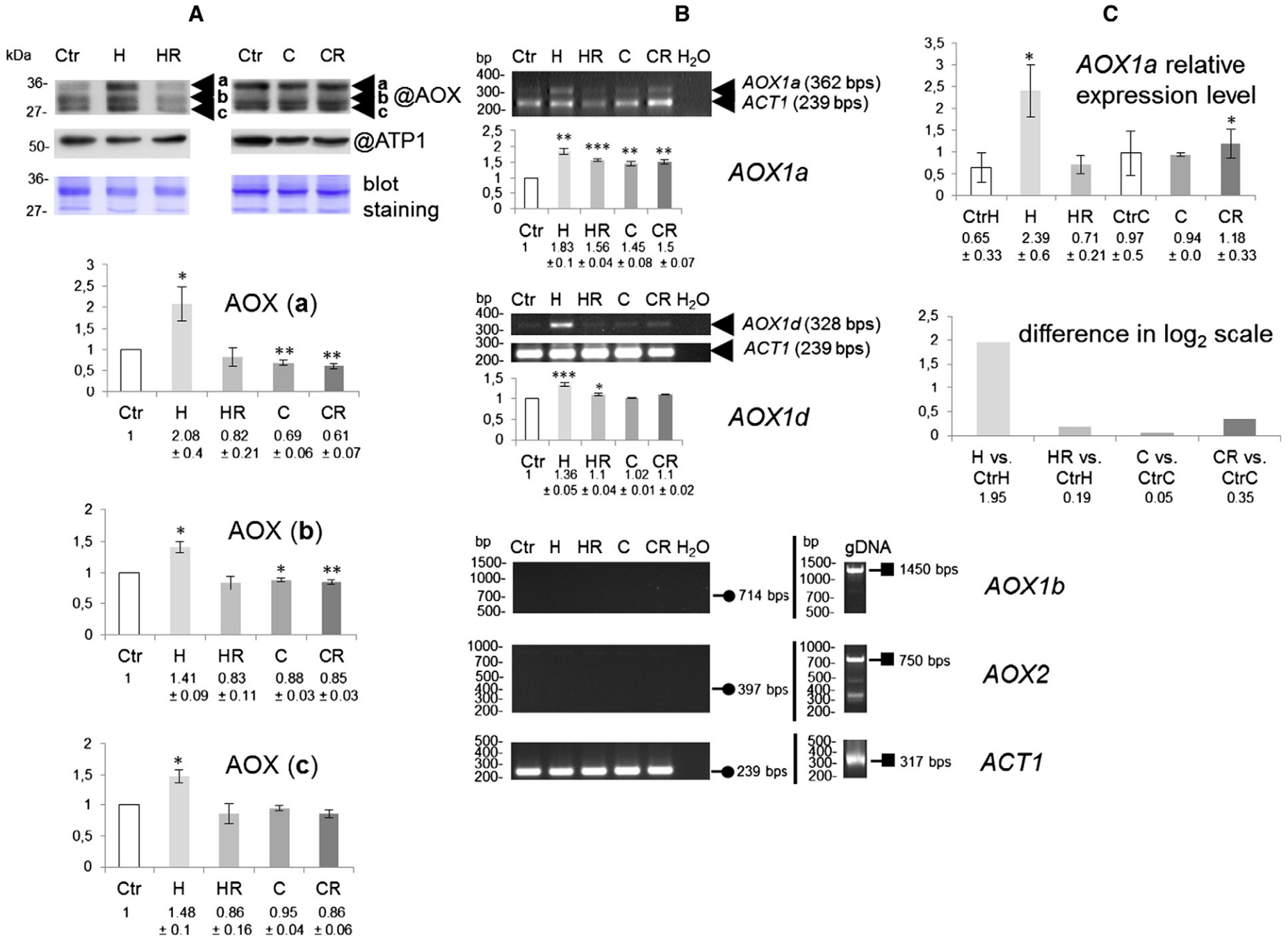
A
kDa Ctr H HR Ctr C CR
36-
27-
a
b
c
@AOX
50-
@ATP1
36-
27-
blot staining
AOX (a)
Ctr H HR C CR
1 2.08 ± 0.4 0.82 ± 0.21 0.69 ± 0.06 0.61 ± 0.07
AOX (b)
Ctr H HR C CR
1 1.41 ± 0.09 0.83 ± 0.11 0.88 ± 0.03 0.85 ± 0.03
AOX (c)
Ctr H HR C CR
1 1.48 ± 0.1 0.86 ± 0.16 0.95 ± 0.04 0.86 ± 0.06
B
bp Ctr H HR C CR H2O
AOX1a (362 bps)
ACT1 (239 bps)
AOX1a
Ctr H HR C CR
1 1.83 ± 0.1 1.56 ± 0.04 1.45 ± 0.08 1.5 ± 0.07
AOX1d (328 bps)
ACT1 (239 bps)
AOX1d
Ctr H HR C CR
1 1.36 ± 0.05 1.1 ± 0.04 1.02 ± 0.01 1.1 ± 0.02
bp Ctr H HR C CR H2O
714 bps
AOX1b
bp gDNA
1450 bps
397 bps
AOX2
750 bps
239 bps
ACT1
317 bps
C
AOX1a relative expression level
CtrH H HR CtrC C CR
0.65 ± 0.33 2.39 ± 0.6 0.71 ± 0.21 0.97 ± 0.5 0.94 ± 0.0 1.18 ± 0.33
difference in log2 scale
H vs. CtrH 1.95
HR vs. CtrH 0.19
C vs. CtrC 0.05
CR vs. CtrC 0.35

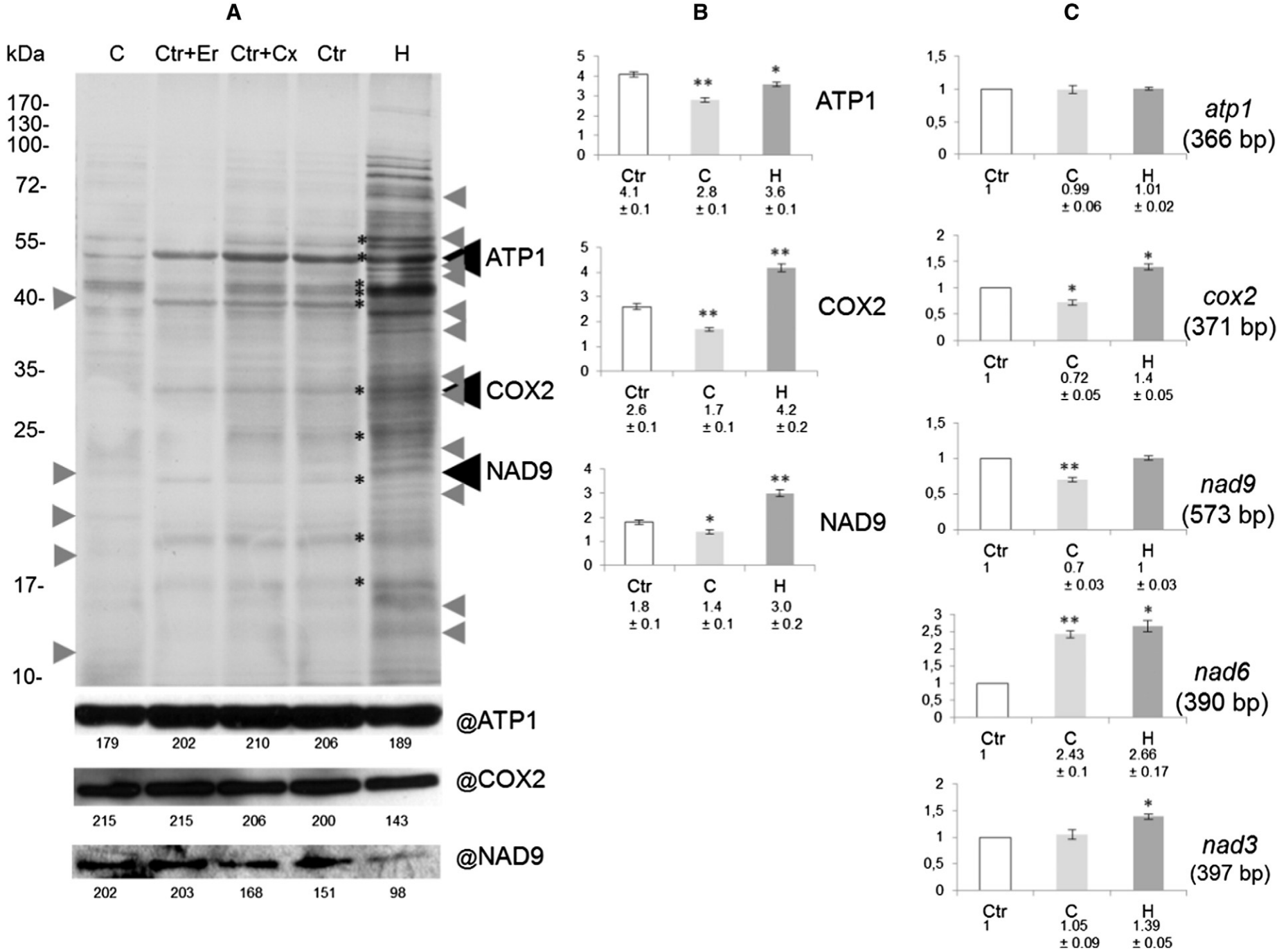
A
kDa
C
Ctr+Er
Ctr+Cx
Ctr
H
170-
130-
100-
72-
55-
40-
35-
25-
17-
10-
ATP1
COX2
NAD9
@ATP1
179 202 210 206 189
@COX2
215 215 206 200 143
@NAD9
202 203 168 151 98
B
ATP1
Ctr 4.1 ± 0.1
C 2.8 ± 0.1
H 3.6 ± 0.1
COX2
Ctr 2.6 ± 0.1
C 1.7 ± 0.1
H 4.2 ± 0.2
NAD9
Ctr 1.8 ± 0.1
C 1.4 ± 0.1
H 3.0 ± 0.2
C
atp1 (366 bp)
Ctr 1
C 0.99 ± 0.06
H 1.01 ± 0.02
cox2 (371 bp)
Ctr 1
C 0.72 ± 0.05
H 1.4 ± 0.05
nad9 (573 bp)
Ctr 1
C 0.7 ± 0.03
H 1 ± 0.03
nad6 (390 bp)
Ctr 1
C 2.43 ± 0.1
H 2.66 ± 0.17
nad3 (397 bp)
Ctr 1
C 1.05 ± 0.09
H 1.39 ± 0.05

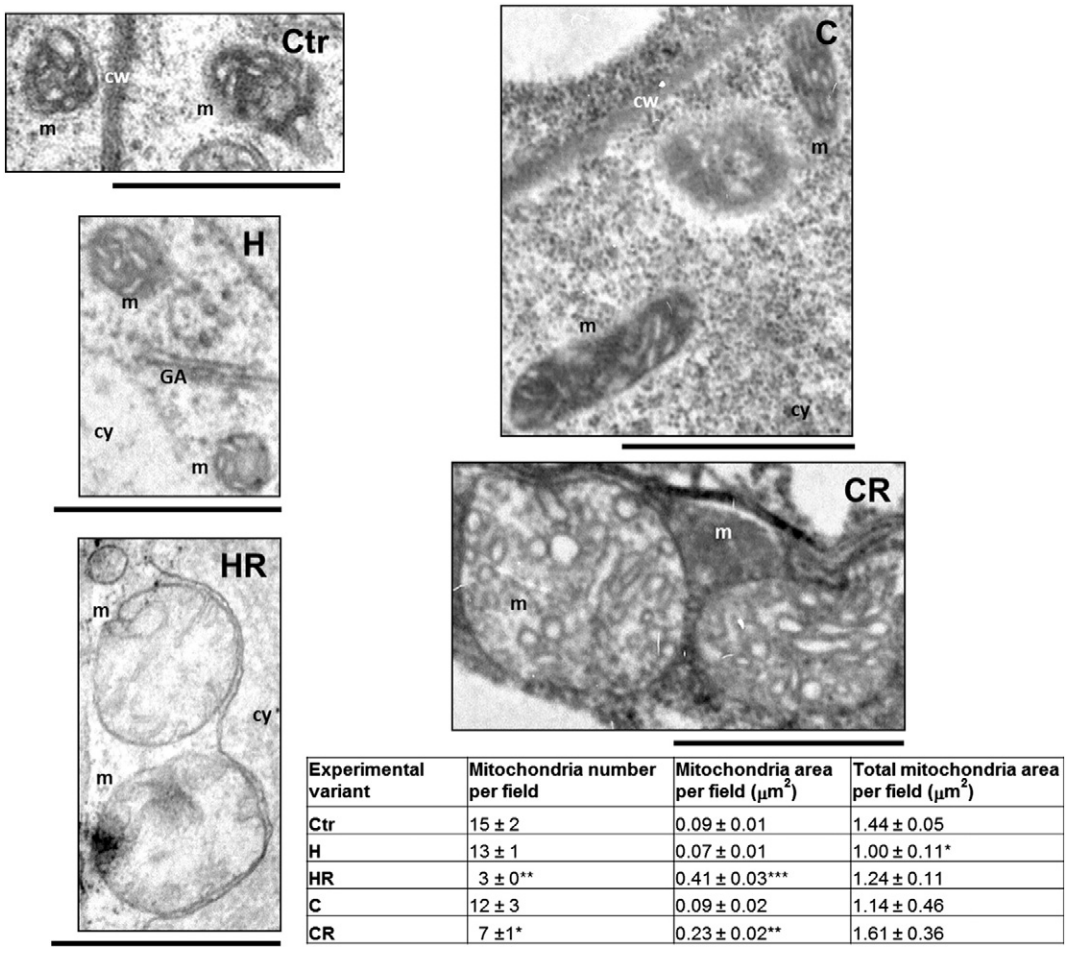

Experimental variant	Mitochondria number per field	Mitochondria area per field (μm^2)	Total mitochondria area per field (μm^2)
Ctr	15 ± 2	0.09 ± 0.01	1.44 ± 0.05
H	13 ± 1	0.07 ± 0.01	1.00 ± 0.11*
HR	3 ± 0**	0.41 ± 0.03***	1.24 ± 0.11
C	12 ± 3	0.09 ± 0.02	1.14 ± 0.46
CR	7 ±1*	0.23 ± 0.02**	1.61 ± 0.36

Fig. 8. Mitochondrial ultrastructure under temperature stress conditions. TEM images from cell sections obtained from the apical layer of cauliflower curds. Material was taken from control plants (Ctr), cold-treated (C) or heat-treated (H) plants and from cold-recovered (CR) and heat-recovered (HR) plants. Scale bars below each image represent 1 μm. cy, cytoplasm; cw, cell wall; GA, Golgi cisterns; m, mitochondria. For each experimental variant, quantification of mitochondrial number as well as the average area occupied by a single mitochondrion and the area occupied by all mitochondria in given TEM micrograph field (in μm^2) was displayed in the accessory table. ***, $p < 0.001$, **, $p < 0.01$, *, $p < 0.05$ of mean (± S.E.) versus control values.

isoforms resulting from the expression of *AOX* gene family and diverse posttranslational modifications of the protein (Fig. 6). The estimated molecular mass values of these polypeptides are similar to previously reported data [21,30]. As shown in Fig. 6A, a significant increase in the accumulation of all AOX polypeptides (ca. 1.4–2-fold change) was revealed only after heat stress. This result is consistent with measurements of the cyanide-resistant respiration (Table 4). Strikingly, after cold stress and cold recovery, a general decline in AOX abundance was observed (except AOX band *c*) (Fig. 6A). In particular cases, AOX may not be upregulated at the protein level by chilling [72,90]. Again, measurements of cyanide-resistant respiration (Table 4) are consistent with the AOX abundance profile. The lowest unstimulated and pyruvate-stimulated activities of AOX are evident in cold (Table 4). However, after cold recovery, despite no apparent increase in AOX abundance (Fig. 6A), an intermediate pyruvate-stimulated AOX activity was observed, that was slightly increased compared to the control and strongly reduced compared to the heat-treated samples (Table 4). A similar phenomenon, i.e., an increase in AOX activity despite the lack of an increase in protein abundance, has been previously reported [3]. Temperature stress may also lead to the AOX regulation in certain species within the same genus [29]. Interestingly, in tobacco (*Nicotiana tabacum*) leaves, AOX abundance reached a maximum after 48 h of cold treatment and slowly decreased afterwards [99]. In turn, in Arabidopsis leaves, the AOX abundance is not affected by temperature changes, but a short one-day chilling transiently increases AOX activity [3].

We also checked whether transcriptomic changes accompany the AOX protein alterations. Primers specific for the amplification of cauliflower homologs of Arabidopsis *AOX* transcripts (*AOX1a*, *AOX1b*, *AOX1d* and *AOX2*) were used (Supplementary Table 1). Due to the insufficient data representing *Brassica* ESTs and reference RNA sequences, we were unable to amplify *AOX1c* mRNA. Cauliflower *AOX1a* and *ACT1* cDNA partial sequences were cloned and deposited in GenBank (accession numbers KC631778 and KC631780). The respective genomic

Fig. 7 Mitochondrial translation in cauliflower mitochondria under temperature stress. (A) The profile of [^{35}S]-Met-labeled proteins during *in organello* translation using mitochondria. The image was obtained after a rtg film exposure on the blot with proteins transferred after SDS-PAGE. For protein size calibration, the PageRuler Prestained Protein Ladder (Thermo Scientific) was used. Protein molecular mass is indicated in kDa. Black arrowheads mark the positions of ATP1, COX2 and NAD9 proteins. Gray arrowheads indicate the position of diversely labeled proteins under stress conditions. Asterisks mark highly labeled proteins in the control. At the bottom, a Western blot analysis of selected mitochondrial proteins on the same blot is shown. Antibodies against ATP synthase subunit-α (@ATP1), the COX2 subunit of CIV (@COX2) and the NAD9 subunit of CI (@NAD9) were used. Values below each signal refer to the densitometric volumes of each protein. (B) The relative ratio (in %) of the densitometric volume of radiolabeled ATP1, NAD9 and COX2 signals to the densitometric volume of all labeled protein pools in control and after temperature stress. The mean values (± S.E.) are shown. (C) The relative level of cauliflower *atp1*, *cox2*, *nad9*, *nad6* and *nad3* transcripts determined by semi-q-RT-PCR. For normalization, cauliflower *actin*1 was amplified as an internal control. Mean values (± S.E.) were standardized relative to the control (set to 1.00). Ctr, control; Ctr + Er, control + erythromycin; Ctr + Cx, control + cycloheximide; C, cold stress; H, heat stress. **, $p < 0.01$, *, $p < 0.05$ versus control values.

sequence fragments are provided under accession numbers KC631779 and KC631781. Using RT-PCR in semiquantitative (semi-q-RT-PCR) and q-RT-PCR assays (with a cauliflower *ACT1* mRNA fragment as an internal standard) (Figs. 6B, *top*, and 6C), we noted changes in the accumulation of *AOX1a* transcripts encoding the AOX isoform that is frequently affected by abiotic stress [17]. The expression of the *AOX1a* gene at the transcriptional level was significantly increased under heat stress similarly to the alterations in the protein level (Figs. 6B, *top*, and 6C). In addition, after cold recovery *AOX1a* mRNA abundance was slightly but significantly increased and exceeded the protein level, which is a known phenomenon for plant transcriptome encoding for mitochondrial proteins [94]. Watanabe et al. [100] showed that out of the whole gene family, only the abundance of *AOX1a* transcripts increased during the first 10 h of cold treatment in Arabidopsis plants and decreased afterwards. In our study, the accumulation of AOX isoforms and *AOX1a* mRNA was assayed after 10 days of the same temperature conditions, which may explain the less evident effects. In cauliflower curds, contrary to the *AOX1a* expression profile, the up-regulation of *AOX1d* transcripts investigated by semi-q-RT-PCR was noticed both in heat and heat recovery (Fig. 6B, *middle*). Unfortunately, despite a high specificity of primers, which were designed for amplification of cauliflower *AOX1b* and *AOX2* genomic sequences, no cDNA products of expected size (714 and 397 bp, respectively) were obtained. This observation suggests that these transcripts are accumulated at very low levels in cauliflower curds (Fig. 6B, *bottom*). Overall, heat stress resulted in the increased AOX protein and *AOX1a* and *AOX1d* mRNA abundances (Fig. 6A, B). AOX transcripts have also been shown to be specifically up-regulated after heat and severe heat treatment in Arabidopsis leaves [73] and after a combination of drought and heat stresses in both tobacco [79] and Arabidopsis leaves [73].

On the whole, cauliflower AOX differentially participates in the response to various temperature stress conditions. In heat treatment, the increase occurred in the levels of the *AOX1a* and *AOX1d* transcripts, and AOX protein. However, in heat recovery and cold recovery, an adaptive over-accumulation of *AOX1a* and *AOX1d* messengers (respectively) was observed, which was partially accompanied by the decrease in protein abundance (Fig. 6A, B). These results emphasize the relevance of stress recovery phase for the regulation of AOX expression. Overall, the changes of AOX activity could be controlled independent of protein abundance, e.g., by a post-translational biochemical activation and the regulation of transcript pool, which is accessible for protein synthesis from diverse AOX genes.

3.7. Mitochondrial translation is significantly affected in cold and heat stress

To extend our data on cauliflower mitochondrial biogenesis under temperature stress, we inspected mitochondrial translation by carrying out *in organello* assays. Following cold methionine chase after *in organello* protein labeling, SDS-PAGE, Western blotting and autoradiography revealed highly labeled polypeptides in mitochondria from control plants (marked by asterisks in Fig. 7A). The [^{35}S] methionine incorporation pattern remained largely unaffected in lines containing cytosolic (6 mM cycloheximide) and plastid (12 mM erythromycin) protein synthesis inhibitors (Fig. 7A), indicating the purity of the mitochondrial preparations.

We observed some qualitative differences in the profiles of newly synthesized mitochondrial polypeptides between control and stressed plants (marked by gray arrowheads on Fig. 7A). Strikingly, [^{35}S] methionine incorporation was more efficient in heat than cold stress. The inhibitory effects of cold treatment on plant protein synthesis have been observed previously [31]. Nebiolo and White [63] have demonstrated that the efficiency of [^{35}S] methionine incorporation into preheated maize (*Zea mays*) mitochondria is affected. Labeling of intact rice (*Oryza sativa*) leaves with [^{35}S] methionine and SDS-PAGE revealed polypeptides with a diverse labeling efficiency in cold [33]. Contrary to our findings, *in organello* synthesis in Arabidopsis mitochondria from sucrose-depleted cultures was unaffected [27]. Therefore, only selected abiotic stresses in selected experimental models may affect mitochondrial protein synthesis.

We estimated the relative contribution of radioactivity associated with immunodetected proteins (including the ATP1 subunit of ATP synthase, the NAD9 subunit of CI and the COX2 subunitof CIV) in a total labeled protein pool by densitometry (Fig. 7A, B). In order to distinguish between specific aberrations in mitochondrial translation and changes in labeled pools of individual mitochondrial proteins that resulted from accompanying transcript alterations, we monitored the level of some mitochondrial mRNAs by semi-q-RT-PCR (Fig. 7C). We noticed a decrease in the level of *de novo* synthesized ATP1, COX2 and NAD9 polypeptides in cold treatment and additionally, a decrease in the radiolabeled ATP1 level after heat treatment, most likely because of stress-induced protein degradation or perturbations in proteins synthesis [33]. In cauliflower mitochondria, subunit-α of ATP synthase was labeled with high efficiency. However, the only decrease in the *de novo* synthesized ATP1 pool in cold and heat could be attributed to the translation impairments, because changes in COX2 and NAD9 proteins in stress roughly accompanied transcript variations in mitochondria used for *in vitro* translation (Fig. 7B, C). Surprisingly, three investigated *nad* messengers (*nad*3, *nad*6 and *nad*9) showed diverse levels of accumulation in investigated stress conditions (Fig. 7C, *bottom*). Basing on the previously discussed data [94], a more coordinated expression of the genes encoding for the same protein complex subunits and belonging to the same functional category was expected.

The sensitivity of ATP synthase synthesis to temperature stress parallels our DIGE data, indicating that heat affected the biogenesis of ATP synthase and that the process was not repaired in the course of recovery (Section 3.3). Alterations in cauliflower mitochondrial translation might be a part of an adaptive response due to the diverse susceptibility of respiratory chain components to temperature stress (Sections 3.2 and 3.3). Overall, the affected synthesis of certain mitochondrial proteins (especially ATP1) accompanied changes in accumulation in the total protein pool, which contribute for changes in cauliflower mitochondrial biogenesis under temperature stress conditions.

3.8. The ultrastructure of cauliflower curd mitochondria is affected only after stress recovery

Numerous changes in mitochondrial morphology and ultrastructure are present under various environmental stimuli [18,53,62]. The number of mitochondria inside plant cells may be affected by [68]. To estimate whether molecular alterations were accompanied by an affected mitochondrial morphology, we studied the cell ultrastructure from an apical layer of cauliflower curds by transmission electron microscopy. Using ImageJ, we counted mitochondrial number per field and calculated the area occupied by all mitochondria as well as by the single mitochondrion per field (Fig. 8). Mitochondrial morphology from the apical layer of cauliflower curds grown in control conditions was consistent with our previous results [81]. The mitochondria appeared as oval, ellipsoid or often bent rod-like organelles, with a dense matrix and club-shaped cristae (Fig. 8). In heat or cold stress, the number of mitochondria and the mitochondrial area were not affected. Strikingly, the mitochondrial ultrastructure of cauliflower mitochondria was significantly altered only after stress recovery. This alternation was accompanied by an evident decrease in the mitochondrial number and by swelling, as the area occupied by a single mitochondrion significantly increased. In cold recovery, cristae swelling was particularly visible; however, during heat recovery cristae disappeared. In heat recovery, an internal translucence was also noticed. In addition, vesicular structures were present within the mitochondria of cold-

recovered cauliflower plants. After stress recovery, the mitochondria were enclosed by membranous whorls. Similar phenomena were reported for mitochondria from mung bean (*Vigna radiate*) and cucumber (*Cucumis sativus*) [42,53].

We speculate that the phenomena observed in our study may be associated with an induction of programmed cell death [78]. However, we were unable to detect electron-dense particles in cauliflower curd mitochondria from heat-stressed or heat-recovered plants, which has been reported previously for other species [101]. Our results are also similar to the chill recovery responses of *Episcia reptans*, in which mitochondria were disorganized [62]. Conversely, Vella et al. [97] reported that after a prolonged (72 h) chilling, mitochondria from Arabidopsis mesophyll cells were aberrant; however, after recovery, the mitochondrial morphology was well preserved. Additionally, mild heat shock conditions (similar to those in our study) did not disturb tomato (*Lycopersicon esculentum*) mitochondria [65]. On the contrary, cauliflower mitochondria responded in a different manner. In cold and heat recovery (contrary to the impact of cold and heat stress), the mitochondrial ultrastructure in cauliflower curds was affected. This phenomenon may be the consequence of the high sensitivity of this organ to a shift from temperature stress to control conditions. However, functional studies indicate that the integrity of outer mitochondrial membrane was preserved among all preparations of isolated mitochondria (Table 4). Contrary to Arabidopsis, cauliflower is only partially adapted to temperature stress [14,32]. In the future, we will elucidate whether cauliflower mitochondria contribute to organellar relocation under stress and in stress recovery, using fusion proteins targeted to mitochondria and fluorescent staining.

4. Conclusions

Cauliflower mitochondria are actively engaged in the response to various temperature treatments. We would like to emphasize that (i) despite new alterations in the levels of respiratory proteins described in our study, the OXPHOS architecture and interactions between some Cs were unexpectedly stable in heat and after heat recovery, refuting a more dynamic status of matrix Cs. (ii) In stress, the decreased *in-gel* activity of selected mitochondrial Cs was not repaired during stress recovery, when ultrastructural alterations (including swelling) take place. (iii) The activity of mitochondrial respiratory chain and ATP synthesis yield were affected most likely due to changes in AOX activity. In general, heat stress resulted in lowered OXPHOS efficiency, while cold stress improved it. (iv) The diverse AOX activity (a cyanide-resistant respiration) was accompanied by changes in AOX protein accumulation. Contrary to cold, heat stress induced an increase in AOX activity and protein levels, while heat recovery reversed these changes. (v) The overall capacity of mitochondrial translation and the synthesis of ATP synthase subunit were affected and accompanied by the low coordination of mitochondrial gene transcriptional responses to cold and heat.

In general, proteomic changes in stress recovery were accompanied by selected physiological (functional) and ultrastructural alterations. Although, multiple steps of coordination of cauliflower mitochondrial biogenesis in cold and heat and stress recovery have been proposed, they do not contribute equally to this multistep and complex process. A limited control of mitochondrial biogenesis during the stress and stress recovery included not only aberrations in Cs assembly/disassembly (a key regulatory step in organellar biogenesis) [27], but also translation impairments and structural as well as activity responses (major alterations in the respiratory chain complex subunits, AOX, matrix enzymes and protein import system). Thus, this study significantly extends our understanding of plant mitochondrial biogenesis under environmental conditions (Supplementary Fig. 4).

Supplementary data to this article can be found online at http://dx.doi.org/10.1016/j.bbabio.2015.01.005.

Acknowledgements

We are very grateful to Hans-Peter Braun, Dagmar Lewejohann and Jennifer Klodmann (Institute for Plant Genetics, Leibniz Universität Hannover, Germany) as well as Christina Lebing and Markus Kolbe (DECODON GmbH, Germany) for the help with DIGE and protein identifications. We thank the staff of Electron and Confocal Microscopy and Molecular Biology Techniques Laboratories (Faculty of Biology, Adam Mickiewicz University in Poznan, Poland) for the help in microscopic and q-RT-PCR analyses. We are grateful Wlodzimierz Krzesinski and Tomasz Spizewski (University of Life Sciences, Poznan, Poland) for cauliflower cultivation and the help in physiological assays. This work was supported by the Ministry of Science and Higher Education, Poland, grant no. N N303 338835 for M.R (resources for science in 2008–2010) and KNOW Poznan RNA Centre, 01/KNOW2/2014.

References

[1] A.J. Alverson, D.W. Rice, S. Dickinson, K. Barry, J.D. Palmer, Origins and recombination of the bacterial-sized multichromosomal mitochondrial genome of cucumber, Plant Cell 23 (2011) 2499–2513.
[2] S. Amme, A. Matros, B. Schlesier, H.-P. Mock, Proteome analysis of cold stress response in *A. thaliana* using DIGE-technology, J. Exp. Bot. 57 (2006) 1537–1546.
[3] A.F. Armstrong, M.R. Badger, D.A. Day, M.M. Barthet, P.M.C. Smith, A.H. Millar, J. Whelan, O.K. Atkin, Dynamic changes in the mitochondrial electron transport chain underpinning cold acclimation of leaf respiration, Plant Cell Environ. 31 (2008) 1156–1169.
[4] O.K. Atkin, Q. Zhang, J.T. Wiskich, Effect of temperature on rates of alternative and cytochrome pathway respiration and their relationship with the redox poise of the quinone pool, Plant Physiol. 128 (2002) 212–222.
[5] J.W. Back, M.A. Sanz, L. De Jong, L.J. De Koning, L.G.J. Nijtmans, C.G. De Koster, L.A. Grivell, H. Van Der Spek, A.O. Muijsers, A structure for the yeast prohibitin complex: structure prediction and evidence from chemical crosslinking and mass spectrometry, Protein Sci. 11 (2002) 2471–2478.
[6] A. Bagniewska-Zadworna, E. Zenkteler, P. Karolewski, M. Zadworny, Phenolic compound localisation in *Polypodium vulgare* L. rhizomes after mannitol-induced dehydration and controlled desiccation, Plant Cell Rep. 27 (2008) 1251–1259.
[7] N. Banzet, C. Richaud, Y. Deveaux, M. Kazmaier, J. Gagnon, C. Triantaphylidès, Accumulation of small heat shock proteins, including mitochondrial HSP22, induced by oxidative stress and adaptive response in tomato cells, Plant J. 13 (1998) 519–527.
[8] J. Bardel, M. Louwagie, M. Jaquinod, A. Jourdain, S. Luche, T. Rabilloud, D. Macherel, J. Garin, J. Bourguignon, A survey of the plant mitochondrial proteome in relation to development, Proteomics 2 (2002) 880–898.
[9] P. Barreto, V.K. Okura, I.A.P. Neshich, I.de G. Maia, P. Arruda, Overexpression of UCP1 in tobacco induces mitochondrial biogenesis and amplifies a broad stress response, BMC Plant Biol. 14 (2014) 144.
[10] D.G. Bernard, Y. Cheng, Y. Zhao, J. Balk, An allelic mutant series of *ATM3* reveals its key role in the biogenesis of cytosolic iron-sulfur proteins in Arabidopsis, Plant Physiol. 151 (2009) 590–602.
[11] J. Borecký, A.E. Vercesi, Plant uncoupling mitochondrial protein and alternative oxidase: energy metabolism and stress, Biosci. Rep. 25 (2005) 271–286.
[12] M. Boutry, M. Briquet, Mitochondrial modifications associated with the cytoplasmic male sterility in faba beans, Eur. J. Biochem. 127 (1982) 129–135.
[13] J.B. Bultema, H.-P. Braun, E.J. Boekema, R. Kouril, Megacomplex organization of the oxidative phosphorylation system by structural analysis of respiratory supercomplexes from potato, Biochim. Biophys. Acta 1787 (2009) 60–67.
[14] J.A. Bunce, Acclimation of photosynthesis to temperature in *Arabidopsis thaliana* and *Brassica oleracea*, Photosynthetica 46 (2008) 517–524.
[15] J.E. Carre, C. Affourtit, A.L. Moore, Interaction of purified alternative oxidase from thermogenic *Arum maculatum* with pyruvate, FEBS Lett. 585 (2011) 397–401.
[16] R. Clifton, R. Lister, K.L. Parker, P.G. Sappl, D. Elhafez, A.H. Millar, D.A. Day, J. Whelan, Stress-induced co-expression of alternative respiratory chain components in *Arabidopsis thaliana*, Plant Mol. Biol. 58 (2005) 193–212.
[17] R. Clifton, A.H. Millar, J. Whelan, Alternative oxidases in *Arabidopsis*: a comparative analysis of differential expression in the gene family provides new insights into function of non-phosphorylating bypasses, Biochim. Biophys. Acta 1757 (2006) 730–741.
[18] I. Couée, S. Defontaine, J.P. Carde, A. Pradet, Effects of anoxia on mitochondrial biogenesis in rice shoots: modification of *in organello* translation characteristics, Plant Physiol. 98 (1992) 411–421.
[19] S. Cui, F. Huang, J. Wang, X. Ma, Y. Cheng, J. Liu, A proteomic analysis of cold stress responses in rice seedlings, Proteomics 5 (2005) 3162–3172.
[20] C.A. Downs, S.A. Heckathorn, The mitochondrial small heat-shock protein protects NADH:ubiquinone oxidoreductase of the electron transport chain during heat stress in plants, FEBS Lett. 430 (1998) 246–250.
[21] T.E. Elthon, R.L. Nickels, L. McIntosh, Monoclonal antibodies to the alternative oxidase of higher plant mitochondria, Plant Physiol. 89 (1989) 1311–1317.
[22] M.L. Escobar Galvis, S. Marttila, G. Håkansson, J. Forsberg, C. Knorpp, Heat stress response in pea involves interaction of mitochondrial nucleoside diphosphate kinase with a novel 86-kilodalton protein, Plant Physiol. 126 (2001) 69–77.

[23] H. Eubel, J. Heinemeyer, H.-P. Braun, Identification and characterization of respirasomes in potato mitochondria, Plant Physiol. 134 (2004) 1450–1459.
[24] H. Eubel, L. Jänsch, H.-P. Braun, New insights into the respiratory chain of plant mitochondria. Supercomplexes and a unique composition of complex II, Plant Physiol. 133 (2003) 274–286.
[25] C.G. Gammulla, D. Pascovici, B.J. Atwell, P.A. Haynes, Differential proteomic response of rice (*Oryza sativa*) leaves exposed to high- and low-temperature stress, Proteomics 11 (2011) 2839–2850.
[26] D.A. Geisler, C. Päpke, T. Obata, A. Nunes-Nesi, A. Matthes, K. Schneitz, E. Maximova, W.L. Araújo, A.R. Fernie, S. Persson, Downregulation of the δ-subunit reduces mitochondrial ATP synthase levels, alters respiration, and restricts growth and gametophyte development in *Arabidopsis*, Plant Cell 24 (2012) 2792–2811.
[27] P. Giegé, L.J. Sweetlove, V. Cognat, C.J. Leaver, Coordination of nuclear and mitochondrial genome expression during mitochondrial biogenesis in *Arabidopsis*, Plant Cell 17 (2005) 1497–1512.
[28] P. Giegé, L.J. Sweetlove, C.J. Leaver, Identification of mitochondrial protein complexes in *Arabidopsis* using two-dimensional blue-native polyacrylamide gel electrophoresis, Plant Mol. Biol. Rep. 21 (2003) 133–144.
[29] M.A. Gonzalez-Meler, M. Ribas-Carbo, L. Giles, J.N. Siedow, The effect of growth and measurement temperature on the activity of the alternative respiratory pathway, Plant Physiol. 120 (1999) 765–772.
[30] O.I. Grabelnych, O.N. Sumina, S.P. Funderat, T.P. Pobezhimova, V.K. Voinikov, A.V. Kolesnichenko, The distribution of electron transport between the main cytochrome and alternative pathways in plant mitochondria during short-term cold stress and cold hardening, J. Therm. Biol. 29 (2004) 165–175.
[31] C.L. Guy, D. Haskell, Induction of freezing tolerance in spinach is associated with the synthesis of cold acclimation induced proteins, Plant Physiol. 84 (1987) 872–878.
[32] F. Hadi, M. Gilpin, M.P. Fuller, Identification and expression analysis of CBF/DREB1 and COR15 genes in mutants of *Brassica oleracea var. botrytis* with enhanced proline production and frost resistance, Plant Physiol. Biochem. 49 (2011) 1323–1332.
[33] M. Hahn, V. Walbot, Effects of cold-treatment on protein synthesis and mRNA levels in rice leaves, Plant Physiol. 91 (1989) 930–938.
[34] C.A. Hamilton, A.G. Good, G.J. Taylor, Induction of vacuolar ATPase and mitochondrial ATP synthase by aluminum in an aluminum-resistant cultivar of wheat, Plant Physiol. 125 (2001) 2068–2077.
[35] J.L. Heazlewood, K.A. Howell, J. Whelan, A.H. Millar, Towards an analysis of the rice mitochondrial proteome, Plant Physiol. 132 (2003) 230–242.
[36] J.L. Heazlewood, J. Whelan, A.H. Millar, The products of the mitochondrial *orf25* and *orfB* genes are Fo components in the plant F_1Fo ATP synthase, FEBS Lett. 540 (2003) 201–205.
[37] J. Heinemeyer, B. Scheibe, U.K. Schmitz, H.-P. Braun, Blue native DIGE as a tool for comparative analyses of protein complexes, J. Proteome 72 (2009) 539–544.
[38] J. Heukeshoven, R. Dernick, Improved silver staining procedure for fast staining in PhastSystem development unit. I. Staining of sodium dodecyl sulfate gels, Electrophoresis 9 (1988) 28–32.
[39] R.C. Holtzapffel, J. Castelli, P.M. Finnegan, A.H. Millar, J. Whelan, D.A. Day, A tomato alternative oxidase protein with altered regulatory properties, Biochim. Biophys. Acta 1606 (2003) 153–162.
[40] K.A. Howell, K. Cheng, M.W. Murcha, L.E. Jenkin, A.H. Millar, J. Whelan, Oxygen initiation of respiration and mitochondrial biogenesis in rice, J. Biol. Chem. 282 (2007) 15619–15631.
[41] S. Huang, N.L. Taylor, R. Narsai, H. Eubel, J. Whelan, A.H. Millar, Functional and composition differences between mitochondrial complex II in *Arabidopsis* and rice are correlated with the complex genetic history of the enzyme, Plant Mol. Biol. 72 (2010) 331–342.
[42] H. Ishikawa, Ultrastructural features of chilling injury: injured cells and the early events during chilling of suspension-cultured mung bean cells, Am. J. Bot. 83 (1996) 825–835.
[43] R.P. Jacoby, A.H. Millar, N.L. Taylor, Investigating the role of respiration in plant salinity tolerance by analyzing mitochondrial proteomes from wheat and a salinity-tolerant amphiploid (wheat × *Lophopyrum elongatum*), J. Proteome Res. 2 (2013) 4807–4829.
[44] C. Jung, C.M. Higgins, Z. Xu, Measuring the quantity and activity of mitochondrial electron transport chain complexes in tissues of central nervous system using blue native polyacrylamide gel electrophoresis, Anal. Biochem. 286 (2000) 214–223.
[45] P. Kieffer, J. Dommes, L. Hoffmann, J.-F. Hausman, J. Renaut, Quantitative changes in protein expression of cadmium-exposed poplar plants, Proteomics 8 (2008) 2514–2530.
[46] T.D. Kjellsen, L. Shiryaeva, W.P. Schröder, G.R. Strimbeck, Proteomics of extreme freezing tolerance in Siberian spruce (*Picea obovata*), J. Proteome 73 (2010) 965–975.
[47] J. Klodmann, M. Senkler, C. Rode, H.-P. Braun, Defining the protein complex proteome of plant mitochondria, Plant Physiol. 157 (2011) 587–598.
[48] J. Klodmann, S. Sunderhaus, M. Nimtz, L. Jänsch, H.-P. Braun, Internal architecture of mitochondrial complex I from *Arabidopsis thaliana*, Plant Cell 22 (2010) 797–810.
[49] R. Kluger, A. Alagic, Chemical cross-linking and protein–protein interactions—a review with illustrative protocols, Bioorg. Chem. 32 (2004) 451–472.
[50] F. Krause, N.H. Reifschneider, D. Vocke, H. Seelert, S. Rexroth, N.A. Dencher, "Respirasome"-like supercomplexes in green leaf mitochondria of spinach, J. Biol. Chem. 279 (2004) 48369–48375.
[51] A. Laisk, Kinetics Of Photosynthesis And Photorespiration In C3-Plants, Nauka, Moscow, 1977.
[52] L. Lamattina, D. Gonzalez, J. Gualberto, J.M. Grienenberger, Higher plant mitochondria encode an homologue of the nuclear-encoded 30-kDa subunit of bovine mitochondrial complex I, Eur. J. Biochem. 217 (1993) 831–838.
[53] S.H. Lee, A.P. Singh, G.C. Chung, Y.S. Kim, I.B. Kong, Chilling root temperature causes rapid ultrastructural changes in cortical cells of cucumber (*Cucumis sativus* L.) root tips, J. Exp. Bot. 53 (2002) 2225–2237.
[54] G. Lenaz, M.L. Genova, Supramolecular organisation of the mitochondrial respiratory chain: a new challenge for the mechanism and control of oxidative phosphorylation, Adv. Exp. Med. Biol. 748 (2012) 107–144.
[55] K. Leonhard, B. Guiard, G. Pellecchia, A. Tzagoloff, W. Neupert, T. Langer, Membrane protein degradation by AAA proteases in mitochondria: extraction of substrates from either membrane surface, Mol. Cell 5 (2000) 629–638.
[56] M.H. Luethy, A. Horak, T.E. Elthon, Monoclonal antibodies to the α- and β-subunits of the plant mitochondrial F_1-ATPase, Plant Physiol. 101 (1993) 931–937.
[57] E.H. Meyer, T. Tomaz, A.J. Carroll, G. Estavillo, E. Delannoy, S.K. Tanz, I.D. Small, B.J. Pogson, A.H. Millar, Remodeled respiration in *ndufs4* with low phosphorylation efficiency suppresses *Arabidopsis* germination and growth and alters control of metabolism at night, Plant Physiol. 151 (2009) 603–619.
[58] J.A. Miernyk, J.J. Thelen, Biochemical approaches for discovering protein–protein interactions, Plant J. 53 (2008) 597–609.
[59] A.H. Millar, H. Eubel, L. Jänsch, V. Kruft, J.L. Heazlewood, H.-P. Braun, Mitochondrial cytochrome *c* oxidase and succinate dehydrogenase complexes contain plant specific subunits, Plant Mol. Biol. 56 (2004) 77–90.
[60] A.H. Millar, J.L. Heazlewood, B.K. Kristensen, H.-P. Braun, I.M. Møller, The plant mitochondrial proteome, Trends Plant Sci. 10 (2005) 36–43.
[61] A.A. Moghadam, S.M. Taghavi, A. Niazi, M. Djavaheri, E. Ebrahimie, Isolation and *in silico* functional analysis of *MtATP6*, a 6-kDa subunit of mitochondrial F1F0-ATP synthase, in response to abiotic stress, Genet. Mol. Res. 11 (2012) 3547–3567.
[62] C. Murphy, J.M. Wilson, Ultrastructural features of chilling-injury in *Episcia reptans*, Plant Cell Environ. 4 (1981) 261–265.
[63] C.M. Nebiolo, E.M. White, Corn mitochondrial protein synthesis in response to heat shock, Plant Physiol. 79 (1985) 1129–1132.
[64] V. Neuhoff, N. Arold, D. Taube, W. Ehrhardt, Improved staining of proteins in polyacrylamide gels including isoelectric focusing gels with clear background at nanogram sensitivity using Coomassie Brilliant Blue G-250 and R-250, Electrophoresis 9 (1988) 255–262.
[65] D. Neumann, K.D. Scharf, L. Nover, Heat shock induced changes of plant cell ultrastructure and autoradiographic localization of heat shock proteins, Eur. J. Cell Biol. 34 (1984) 254–264.
[66] G. Noctor, R. De Paepe, C.H. Foyer, Mitochondrial redox biology and homeostasis in plants, Trends Plant Sci. 12 (2007) 125–134.
[67] T. Obata, A. Matthes, S. Koszior, M. Lehmann, W.L. Araújo, R. Bock, L.J. Sweetlove, A.R. Fernie, Alteration of mitochondrial protein complexes in relation to metabolic regulation under short-term oxidative stress in *Arabidopsis* seedlings, Phytochemistry 72 (2011) 1081–1091.
[68] Y. Ogasawara, K. Ishizaki, T. Kohchi, Y. Kodama, Cold-induced organelle relocation in the liverwort *Marchantia polymorpha* L, Plant Cell Environ. 36 (2013) 1520–1528.
[69] T. Pawlowski, M. Rurek, S. Janicka, K.D. Raczynska, H. Augustyniak, Preliminary analysis of the cauliflower mitochondrial proteome, Acta Physiol. Plant. 27 (2005) 275–281.
[70] K. Peters, M. Niessen, C. Peterhänsel, B. Späth, A. Hölzle, S. Binder, A. Marchfelder, H.-P. Braun, Complex I–complex II ratio strongly differs in various organs of *Arabidopsis thaliana*, Plant Mol. Biol. 79 (2012) 273–284.
[71] K. Pfeiffer, V. Gohil, R.A. Stuart, C. Hunte, U. Brandt, M.L. Greenberg, H. Schägger, Cardiolipin stabilizes respiratory chain supercomplexes, J. Biol. Chem. 278 (2003) 52873–52880.
[72] V.N. Popov, A.C. Purvis, V.P. Skulachev, A.M. Wagner, Stress-induced changes in ubiquinone concentration and alternative oxidase in plant mitochondria, Biosci. Rep. 21 (2001) 369–379.
[73] C.M. Prasch, U. Sonnewald, Simultaneous application of heat, drought, and virus to *Arabidopsis* plants reveals significant shifts in signaling networks, Plant Physiol. 162 (2013) 1849–1866.
[74] G. Qin, X. Meng, Q. Wang, S. Tian, Oxidative damage of mitochondrial proteins contributes to fruit senescence: a redox proteomics analysis, J. Proteome Res. 8 (2009) 2449–2462.
[75] S.J. Ramírez-Aguilar, M. Keuthe, M. Rocha, V.V. Fedyaev, K. Kramp, K.J. Gupta, A.G. Rasmusson, W.X. Schulze, J.T. van Dongen, The composition of plant mitochondrial supercomplexes changes with oxygen availability, J. Biol. Chem. 286 (2011) 43045–43053.
[76] A.G. Rasmusson, A.R. Fernie, J.T. van Dongen, Alternative oxidase: a defence against metabolic fluctuations? Physiol. Plant. 137 (2009) 371–382.
[77] A.G. Rasmusson, K.L. Soole, T.E. Elthon, Alternative NAD(P)H dehydrogenases of plant mitochondria, Annu. Rev. Plant Biol. 55 (2004) 23–39.
[78] E.G. Rikhvanov, K.Z. Gamburg, N.N. Varakina, T.M. Rusaleva, I.V. Fedoseeva, E.L. Tauson, I.V. Stupnikova, A.V. Stepanov, G.B. Borovskii, V.K. Voinikov, Nuclear-mitochondrial cross-talk during heat shock in *Arabidopsis* cell culture, Plant J. 52 (2007) 763–778.
[79] L. Rizhsky, H. Liang, R. Mittler, The combined effect of drought stress and heat shock on gene expression in tobacco, Plant Physiol. 130 (2002) 1143–1151.
[80] C. Rode, M. Senkler, J. Klodmann, T. Winkelmann, H.-P. Braun, GelMap—a novel software tool for building and presenting proteome reference maps, J. Proteome 74 (2011) 2214–2219.
[81] M. Rurek, Diverse accumulation of several dehydrin-like proteins in cauliflower (*Brassica oleracea* var. *botrytis*), *Arabidopsis thaliana* and yellow lupin (*Lupinus luteus*) mitochondria under cold and heat stress, BMC Plant Biol. 10 (2010) 181.

[82] M. Rurek, Plant mitochondria under a variety of temperature stress conditions, Mitochondrion 19 (2014) 289–294.
[83] H. Schägger, G. von Jagow, Tricine-sodium dodecyl sulfate-polyacrylamide gel electrophoresis for the separation of proteins in the range from 1 to 100 kDa, Anal. Biochem. 166 (1987) 368–379.
[84] U.G. Schmidt, A. Endler, S. Schelbert, A. Brunner, M. Schnell, H.E. Neuhaus, D. Marty-Mazars, F. Marty, S. Baginsky, E. Martinoia, Novel tonoplast transporters identified using a proteomic approach with vacuoles isolated from cauliflower buds, Plant Physiol. 145 (2007) 216–229.
[85] H. Seelert, N.A. Dencher, ATP synthase superassemblies in animals and plants: two or more are better, Biochim. Biophys. Acta 1807 (2011) 1185–1197.
[86] G. Sinvany-Villalobo, O. Davydov, G. Ben-Ari, A. Zaltsman, A. Raskind, Z. Adam, Expression in multigene families. Analysis of chloroplast and mitochondrial proteases, Plant Physiol. 135 (2004) 1336–1345.
[87] L.J. Sweetlove, J.L. Heazlewood, V. Herald, R. Holtzapffel, D.A. Day, C.J. Leaver, A.H. Millar, The impact of oxidative stress on *Arabidopsis* mitochondria, Plant J. 32 (2002) 891–904.
[88] Y.-F. Tan, A.H. Millar, N.L. Taylor, Components of mitochondrial oxidative phosphorylation vary in abundance following exposure to cold and chemical stresses, J. Proteome Res. 11 (2012) 3860–3879.
[89] N.L. Taylor, D.A. Day, A.H. Millar, Environmental stress causes oxidative damage to plant mitochondria leading to inhibition of glycine decarboxylase, J. Biol. Chem. 277 (2002) 42663–42668.
[90] N.L. Taylor, J.L. Heazlewood, D.A. Day, A.H. Millar, Differential impact of environmental stresses on the pea mitochondrial proteome, Mol. Cell. Proteomics 4 (2005) 1122–1133.
[91] N.L. Taylor, J.L. Heazlewood, A.H. Millar, The *Arabidopsis thaliana* 2-D gel mitochondrial proteome: refining the value of reference maps for assessing protein abundance, contaminants and post-translational modifications, Proteomics 11 (2011) 1720–1733.
[92] N.L. Taylor, Y.-F. Tan, R.P. Jacoby, A.H. Millar, Abiotic environmental stress induced changes in the *Arabidopsis thaliana* chloroplast, mitochondria and peroxisome proteomes, J. Proteome 72 (2009) 367–378.
[93] A. Urantowka, C. Knorpp, T. Olczak, M. Kolodziejczak, H. Janska, Plant mitochondria contain at least two i-AAA-like complexes, Plant Mol. Biol. 59 (2005) 239–252.
[94] O. Van Aken, B. Zhang, C. Carrie, V. Uggalla, E. Paynter, E. Giraud, J. Whelan, Defining the mitochondrial stress response in *Arabidopsis thaliana*, Mol. Plant 2 (2009) 1310–1324.
[95] R. Van Lis, A. Atteia, G. Mendoza-Hernández, D. González-Halphen, Identification of novel mitochondrial protein components of *Chlamydomonas reinhardtii*. A proteomic approach, Plant Physiol. 132 (2003) 318–330.
[96] G.C. Vanlerberghe, M. Cvetkovska, J. Wang, Is the maintenance of homeostatic mitochondrial signaling during stress a physiological role for alternative oxidase? Physiol. Plant. 137 (2009) 392–406.
[97] N.G.F. Vella, T.V. Joss, T.H. Roberts, Chilling-induced ultrastructural changes to mesophyll cells of *Arabidopsis* grown under short days are almost completely reversible by plant re-warming, Protoplasma 249 (2012) 1137–1149.
[98] J. Velours, P. Paumard, V. Soubannier, C. Spannagel, J. Vaillier, G. Arselin, P.V. Graves, Organization of the yeast ATP synthase F_0: a study based on cysteine mutants, thiol modification and cross-linking reagents, Biochim. Biophys. Acta 1458 (2000) 443–456.
[99] J. Wang, N. Rajakulendran, S. Amirsadeghi, G.C. Vanlerberghe, Impact of mitochondrial alternative oxidase expression on the response of *Nicotiana tabacum* to cold temperature, Physiol. Plant. 142 (2011) 339–351.
[100] C.K. Watanabe, T. Hachiya, I. Terashima, K. Noguchi, The lack of alternative oxidase at low temperature leads to a disruption of the balance in carbon and nitrogen metabolism, and to an up-regulation of antioxidant defence systems in *Arabidopsis thaliana* leaves, Plant Cell Environ. 31 (2008) 1190–1202.
[101] D.L. Webster, K. Watson, Ultrastructural changes in yeast following heat shock and recovery, Yeast 9 (1993) 1165–1175.
[102] I. Wittig, H.-P. Braun, H. Schägger, Blue native PAGE, Nat. Protoc. 1 (2006) 418–428.
[103] S.-P. Yan, Q.-Y. Zhang, Z.-C. Tang, W.-A. Su, W.-N. Sun, Comparative proteomic analysis provides new insights into chilling stress responses in rice, Mol. Cell. Proteomics 5 (2006) 484–496.
[104] G. Yin, H. Sun, X. Xin, G. Qin, Z. Liang, X. Jing, Mitochondrial damage in the soybean seed axis during imbibition at chilling temperatures, Plant Cell Physiol. 50 (2009) 1305–1318.
[105] E. Zerbetto, L. Vergani, F. Dabbeni-Sala, Quantification of muscle mitochondrial oxidative phosphorylation enzymes via histochemical staining of blue native polyacrylamide gels, Electrophoresis 18 (1997) 2059–2064.
[106] M. Zhang, E. Mileykovskaya, W. Dowhan, Cardiolipin is essential for organization of complexes III and IV into a supercomplex in intact yeast mitochondria, J. Biol. Chem. 280 (2005) 29403–29408.
[107] X. Zhang, S. Liu, T. Takano, Overexpression of a mitochondrial ATP synthase small subunit gene (*AtMtATP6*) confers tolerance to several abiotic stresses in *Saccharomyces cerevisiae* and *Arabidopsis thaliana*, Biotechnol. Lett. 30 (2008) 1289–1294.